

RESEARCH ARTICLE

FINITE STRAIN AND KINEMATIC VORTICITY ANALYSIS OF THE ROCKS AS A TOOL TO LOCATE THE THRUSTS FAULTS IN THE HIMALAYAS: A CASE STUDY FROM THE BIRENDRANAGAR-TALPOKHARI AREA OF KARNALI PROVINCE OF NEPAL

Ankit Kandel^a and Kabi Raj Paudyal^{b*}^aNepal Electricity Authority (Soil, Rock, and Concrete Laboratory), Kathmandu, Nepal^bCentral Department of Geology, Tribhuvan University, Kathmandu, Nepal*Corresponding author: paudyalkabi1976@gmail.com

This is an open access article distributed under the Creative Commons Attribution License CC BY 4.0, which permits unrestricted use, distribution, and reproduction in any medium, provided the original work is properly cited.

ARTICLE DETAILS

Article History:

Received 20 October 2023
Revised 04 November 2023
Accepted 15 December 2023
Available online 10 May 2024

ABSTRACT

The Birendranagar-Talpokhari area lies in Surkhet and Dailekh districts of the Karnali Province, Nepal. Geologically, the study area represents parts of the Lesser Himalaya and Sub-Himalaya. The Sub-Himalaya consists of rocks of the Lower Siwalik. The Lesser Himalaya consists of three tectonic units: the Dailekh Group, the Lakharpata Group, and the Surkhet Group. The Dailekh Group is the allochthonous rock unit consisting of sequences of metamorphosed rocks whereas the Lakharpata Group consists of series of carbonate rocks. The Surkhet Group is the para-autochthonous unit consisting of sequences of low-grade metamorphic rocks. The strain ellipsoid of the quartz grains shows the rocks of the Surkhet Group and Dailekh Group bear a differential pattern of deformation. All the samples from the Surkhet Group rocks show the ($R_1 > R_2$) condition whereas the Dailekh Group rocks show the ($R_2 > R_1$) condition. The kinematic vorticity numbers with higher values (sample J19, L5, and M20) are located near the thrust whereas the lower value (sample J19) lies at some distance from the thrust. The simple shear-dominated area is more affected by the shearing effect so that the long axis of the quartz grains gets affected and subjected to rotation during shearing. This result supports the presence of the regional thrusts; (Timile Thrust and Nigalpani Thrust).

KEYWORDS

Finite strain, vorticity, Karnali Province, Nepal

1. INTRODUCTION

The Himalayas was formed by the collision of the Indian Sub-continent with the Eurasian Plate about 55 million years ago (Le Fort, 1975). The northward drift of the Indian plate towards the Eurasian plate is the major cause of the crustal shortening and upliftment of the Himalayas with the development of several thrust faults (Bilham et al., 1997). The Himalayan fold-thrust belt consists of a series of south vagrant thrust systems that have developed in response to the ongoing subduction of the Indian plate beneath the Eurasian plate (Gansser, 1964). The Nepal Himalaya occupies approximately 800 km at the central part of the Himalayan belt out of its 2400 km entire length extending nearly east-west direction. This region is further divided into four different major tectonic units; Sub-Himalaya (Siwalik), Lesser Himalaya, Higher Himalaya, and Tethyan Himalaya from south to north respectively (Gansser, 1964). The collision of India-Eurasia and the continuous movement of the Indian plate towards the Eurasian plate caused the slicing of the rocks into these four blocks along three principal thrusts; the Main Boundary Thrust (MBT), the Main Central Thrust (MCT), and the South Tibetan Detachment System (STDs) from south to north respectively. All these faults converge at one detachment structure along the subduction zone MHT (Ni and Barazangi, 1984). Many works have been carried out in the Lesser Himalaya such as the Nawakot Complex in central Nepal, Nawakot Group, the Tansen Group, and the Kali Gandaki Supergroup in west-central Nepal Dang-Sallayan area in the west Karnali and Dolpo region, etc. (Stöcklin and Bhattarai, 1977; Stöcklin,

1980; Paudyal and Paudel, 2013; Sakai, 1983; 1985; Dhital and Kizaki, 1987; Fuchs, 1974).

Geologically, most of the present study area lies in the Lesser Himalayan zone with some parts of Siwalik in the southern region. Fuchs mapped the large portion of the Lesser Himalayas between the Surkhet and Dailekh districts (Fuchs, 1977). He identified Early Miocene beds (Dagshai or Sutar Formation) at the foot of the Mahabharat Range, in the northern part of Surkhet. He also recognized the thin beds of carbonate (Lakharpata Group) thrust over the Paleocene-Early Eocene strata of the Surkhet Group. Similarly, Dhital described that the geology of the Surkhet-Dailekh area is in the Lesser Himalayan region consisting of three groups: Surkhet Group, Lakharpata Group, and Dailekh Group (Dhital, 2015). The Surkhet Group begins with white-gray-green, thick-bedded quartz arenites or quartzose sandstones, containing shaly intercalations (Melpani Formation). This primarily medium-to coarse-grained arenaceous succession in nature is followed up-section by 150–170 m thick fissile shales (Swat or Subathu Formation). Above the fossiliferous horizon, thick-bedded, medium-grained, compact, gray-green sandstones, regularly alternating with silty and micaceous purple shales or shaly sandstones (Sutar or Dagshai Formation) are present. The Dailekh Group begins with the Ranimatta Formation represented by the moderately to steeply north-dipping sequences of meta basics, alternating mainly with white or some pink quartzite and some phyllites. From north to south Lohore Thrust, Parajul Thrust, Budar Thrust, Garbeta Thrust, and Baddichaur Thrust are present separating one group of lithological succession from another.

Quick Response Code



Access this article online

Website:
www.pakjgeology.com

DOI:
10.26480/pjg.02.2023.56.72

The Birendranagar-Talpokhari area lies in the Surkhet and Dailekh districts of the Karnali Province, Nepal. It lies in the western part of Nepal, which is about 600 km from Kathmandu, Nepal. It is located on the northern hill of the Surkhet Dun Valley. The area is accessible through road by major highways of Nepal. The study area consists of the Churia and Mahabharat regions with a maximum altitude of 2,230 m at Ranimatta and a minimum of 900 m at Baspani Khola. The area shows rugged topography consisting of ridge, spur, saddle, and valley morphology generally with moderate to a very steep slope. The overall drainage pattern of the area is dendritic in nature (Figure 1). The Sot Khola, Itram Khola, and Rati Khola are the major rivers having high gradients with narrow valleys.

The study is focused on the lithostratigraphy in parts of the Surkhet-Dailekh districts aiming to prepare the geological map of the area on a scale of 1:25000. The study of the lithological distribution and its

structures provides first-hand information to assess the study of strain condition and the type of shear component applied on the metamorphosed rock units during deformation.

The main objective of the study is an investigation of the deformation processes to understand the finite strain ellipsoid and the type of shear component applied in different zones of the area. The finite strain ellipsoid and the initial ellipticity can be determined by the R_i/θ method (Ramsay, 1967). Similarly, the type of share component applied during deformation can be determined by Vorticity analysis using the ($R-\theta$) method (Tikoff and Fossen, 1995). The study of kinematic vorticity and strain analysis makes it possible to analyze the deformation characteristics of the tectonically active zone. This type of investigation is the first study in this region.

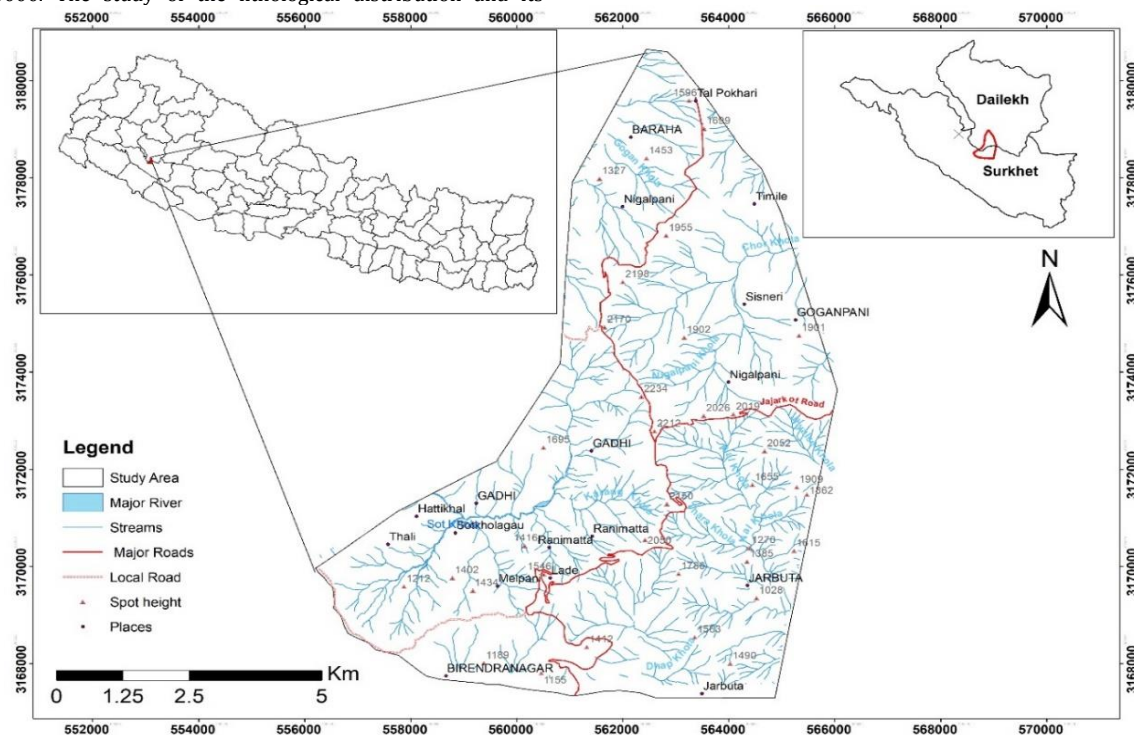


Figure 1: Location map of Birendranagar-Talpokhari area of Surkhet-Dailekh districts

2. METHODOLOGY

2.1 Geological Mapping

The required geological and structural data on the study area were obtained from field observations. The attitude of rocks was identified by measuring the strike/dip of the rocks' bedding plane/foliation plane. The collected data were used for the preparation of a geological map, lithological unit, and their contact relation. The fieldwork was carried out to delineate the stratigraphy and tectonic setting along with the structural data collection. The sampling was based on the relevant traverse in the planned route for the detailed structural analysis to reveal the strain analysis of the area. Representative samples were taken from different exposures systematically. The geological map at the scale of (1:25,000) was prepared by applying mainly two steps: traverse for field observation and at some places following the geological contacts using v's rules.

2.2 Preparation of samples

The samples collected from the study area were prepared for the thin section. Three thin sections from samples A5, A16, and C13 were prepared from the rock units of the Surkhet Group. Samples A5 and A16 belong to the metasandstone of the Malpani Formation whereas sample C13 belongs to the sandstone sample of the Gadhi Formation (upper part of Gadhi Formation). As the different units of this succession consist of differently metamorphosed rocks (lower section consisting of higher grade and upper section consisting of lower grade) the samples were selected to represent the whole sequence. Similarly, thin sections from samples J12, J19, M20, and L5 were prepared from the rock units of the Dailekh Group. Sample J12 and J19 represent the Ranimatta Formation whereas sample M20 and L5 represents the rock units that gets exposed in the Sisneri Formation. Thin sections of the samples were prepared perpendicular to the foliation so that the XY axis of the deformed quartz grains can be measured.

2.3 Finite strain analysis

The deformed and elongated quartz grains were used as strain markers. The Ellipticity (R_i) of each of the grains was calculated by measuring the long axis and the short axis using the software ImageJ. The long axis was divided by the short axis to find out the ellipticity of each of the deformed grains. Along with the measurement of the length of the long axis of the strain ellipse, the orientation angle with respect to the north of the oriented samples was measured. The positive sign ($\theta +ve$) was given to the anticlockwise direction whereas the negative sign ($\theta -ve$) was given to the clockwise direction from the north direction. Each ellipse was plotted as a single point in the (R_i/θ) graph. The long-axis orientation data of each strain ellipse were plotted to find out the average orientation by making the frequency histogram of the θ directions at the interval of 10° for the Surkhet Group rocks and 5° for the Dailekh Group rocks. The point plots in the (R_i/θ) graph were contoured using the kernel density plot using ArcGIS software to find out the maximum density of each of the plots and to find out the fluctuation (F) of the angles. Based on the value of the fluctuation on the (R_i/θ) graph two conditions can be determined (Ramsay, 1967); $R_s > R_i$ if the fluctuation is less than 90° ($F < 90^\circ$) where the data are concentrated on the restricted area of (R_i/θ) graph and $R_s < R_i$ if the fluctuation is greater than 90° and the data plotted are scattered on the greater area of (R_i/θ) graph. The value of R_s and R_i were determined for each of the samples using the expressions formulated by (Ramsay and Huber, 1983).

2.4 Vorticity analysis

To establish the non-linear ratio of pure and simple shear components of deformation kinematic vorticity number was used. The vorticity value of zero ($W_m=0$) represents the pure share condition whereas the vorticity value of one ($W_m=1$) represents the simple shear condition (Means, 1994). The average values of vorticity (W_m) in between these represent the flows between the pure shear and simple shear ($1 > W_m > 0$) known as general

shear (Passchier and Trouw, 2005). For the evaluation of the value of vorticity (W_m), the ($R_f - \theta$) nomogram was used where angle θ is the angular relation between the long axis of the strain ellipsoid and the shear band surface (C-surface) and R_f is the value of Ellipticity (Forte and Bailey, 2007). The shear band C-surface gets preserved in the argillaceous part of the thin section. The angle of fluctuation of quartz grains from the C-surface is plotted against the final Ellipticity R_f of the grains so that the scattered plot of each of the grains can be obtained. These scattered plots were then contoured based on the Kernel Density Plot using Software ArcGIS. The maximum density concentration (peak of the Kernel density plot) was then considered to find the value of Vorticity (W_m). The ($R_f - \theta$) nomogram plot gives the three stages of pure shear, simple shear, and general shear (Forte and Bailey, 2007). If the value of vorticity (W_m) is greater than 0.95 simple shear is dominated (>80%), if it is between 0.3 and 0.95 general shear (both the simple shear and pure shear component) is applied whereas if the value of vorticity (W_m) is less than 0.3 the pure shear is dominated (Forte and Bailey, 2007).

3. RESULTS

3.1 Site geology

The Birendranagar-Talpokhari section of the study area represents major parts of the Lesser Himalaya with some Sub Himalayan sequences. It consists of four major tectonic units: Dailekh Group, Lakharpata Group, Surkhet Group, and Siwalik.

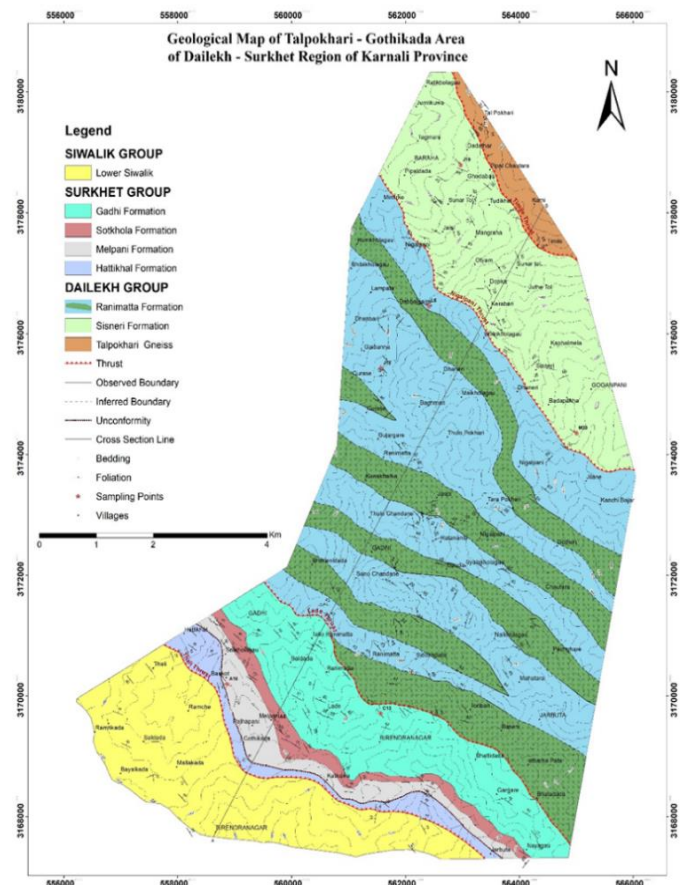
The Dailekh Group is the allochthonous rock unit consisting of sequences of different metamorphosed rocks like phyllite, quartzite, metasandstone, and meta basic rocks (Fuchs, 1974). This Group is thrust over the para-autochthonous rocks units of the Surkhet Group. The Talpokhari Gneiss is the northernmost unit among the Dailekh Group which is thrust over the Sisneri Formation (Figure 2). The thick beds of augen mica-gneiss are found with conspicuous banding structure. It consists of medium to thick successions of augen mica-gneiss with some banded structures. Fuchs mapped this unit as the massive granitic gneiss consisting of coarse-grained porphyritic rocks (Fuchs, 1977). Dhital mapped this unit as the mylonitic gneiss unit. This unit overlies the low-grade country rocks such as the Sisneri Phyllite (Dhital, 2015). The Sisneri Formation is characterized by the presence of a monotonous succession of light grey to dark grey, medium-to coarse-grained metasandstone interbedded with greenish grey to dark grey phyllite. Medium to coarse-grained metasandstone beds consisting of a series of deformed quartz veins are interbedded with some psammitic phyllite. Medium to thick beds of grey-colored metasandstone consists of numerous quartz veins, which get deformed to form boudins and folded veins (Figure 3(A)). This unit is bounded by the northern Timile Thrust and southern Nigalpani Thrust. The Nigalpani Thrust is underlined by the thick succession of the Ranimatta Formation. This unit mainly comprises the metamorphosed rocks of quartzite and phyllite. The basal part of this unit consists of very coarse-grained clastic white quartzite whereas the middle part is composed of parallel-laminated grey to pinkish white quartzites interbedded with sporadic green to light gray bands of phyllite. White to pinkish-white, medium-grained quartzite is intercalated with greenish meta basic rock successions. The upper part of this unit consists of medium-to-fine-grained pale grey to pinkish, white quartzites interbedded with greenish grey phyllite and medium-fine-grained foliated meta basic rocks in equal proportion. This unit is correlated with the Nagthats, particularly those of the Bhowali-Bhim Tal area of Kumaon where the quartzites are similarly associated with basic volcanoes (Fuchs, 1977).

The Lakharpata Group consists of most carbonate rocks interbedded with some shales and other rocks depending on the different lithological Formations. The Hattikhal Formation is the only lithological unit that gets exposed in the study area. This unit consists of light grey to grey laminated limestone with interbedding of thinly laminated greenish-grey shale and dolomite. The lower part of this unit is highly deformed forming red-colored soil intermixing with brecciated and recalcified rock fragments of limestone. Layers of conchoidal fractured greyish to sky blue cherty limestone are interlaminated with pale yellow shales at the middle part of this section. The wavy laminations preserved in limestone beds show the presence of algal structures. Current ripple marks are also preserved in the layers of shales. The upper part of this section consists of light grey dolomites interbedded with layers of limestone and shale. Geological structures like stalactites and stalagmites are formed due to the leaching of high calcium carbonate-containing rocks (Figure 3(B)).

The Surkhet Group is the Para-autochthonous rock unit consisting of normal sequences of low-grade metamorphic rocks with some fossiliferous horizons of the Paleocene to Early Eocene age (Fuchs, 1977). The basal part of this unit is succeeded by the dominance of the arenaceous

rock unit 'Melpani Formation.' This unit comprises mainly gray to dark grey, sometimes white metasandstone interbedded with greenish-grey shale in various proportions. The lower section comprises well-bedded white to greyish white quartz arenite having dominance of medium-coarse-grained arenaceous quartz fragments superior to which medium to thickly bedded medium-grained grey to dark grey ferruginous metasandstone beds intercalated with thin beds of greenish grey shale. About 3.6 m thick band of ferruginous and fossiliferous metasandstone horizon is well mapped at the topmost portion as the marker horizon (Figure 3(C)). This unit resembles the Tal Formation consisting of white gray, green rather thick-bedded quartzite and quartzitic sandstone with shaly intercalations (Fuchs, 1977). The Sotkhola Formation is well exposed over the arenaceous formation. This litho-unit is characterized by the succession of grey to dark-grey fissile shale with some fossiliferous limestone at the upper part. The fossils of bivalves and gastropods are well preserved in the uppermost horizon of limestone, which is well exposed in the Sot Khola section. The lithology of this unit resembles the Subathu Formation consisting of grey-green fissile shale consisting of the fossiliferous limonitic layer (Fuchs, 1977). The uppermost lithological formation of the Surkhet Group that gets exposed over the Sotkhola Formation is the Gadhi Formation. This unit mainly comprises fine-to-medium-grained green, greenish grey to purple sandstone intercalated with purple to red-purple shale. Medium to thickly bedded, medium-to coarse-grained sandstone is interbedded with thinly bedded purple shale. The purple to red-purple shale is dominant over fine-medium-grained purple sandstone with the appearance of a mudball at the lower section. An orthogonal joining pattern is seen in purple sandstone due to the spheroidal weathering developed in the area. This litho-unit resembles the rocks of thick-bedded, medium-grained compact grey-green sandstone alternating with silty and micaceous shales and shaley sandstones of the Dagshai Formation and the Sutar Formation respectively (Fuchs, 1977; Dhital, 2015).

The Siwalik Group is the southernmost lithological unit of the area, which consists of highly weathered sedimentary rock sequences. The Lower Siwalik is the oldest lithological unit among other Siwalik units, which is well exposed in the area. This unit is characterized by the presence of fine-medium-grained, light grey to grey sandstones with lamina intercalated with variegated reddish yellow to pale yellow mudstones. The southern part of the Itram Khola section consists of the alternation of very fine-grained grey sandstone interbedded with layers of mudstone. The bed of sandstone consists of different parts of plant fossils like trunks and leaves (Figure 3(D)). Calcareous mudballs are also preserved in the beds of sandstone in this section.



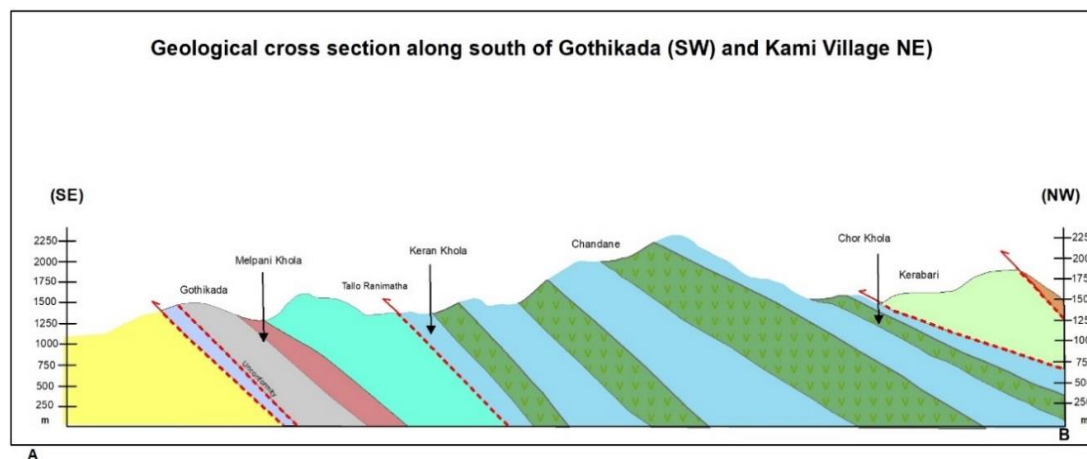


Figure 2: (A) Geological Map of Birendranagar-Talpokhari area of Surkhet-Dailekh Districts. (B) Cross-section through the line A(SE)-B(NW) from Geological Map.

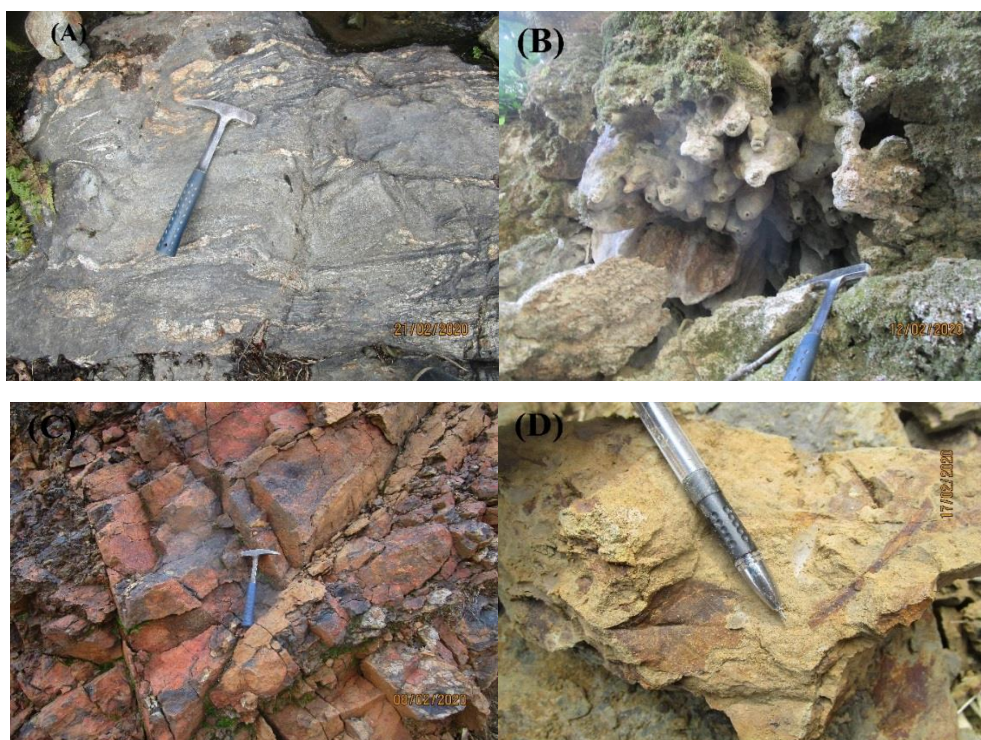


Figure 3: (A) Dark-grey medium-grained metasandstone with quartz vein in Sisneri Formation at Sunar Tol area. (B) Photograph of stalactites observed in the Hattikhal Formation at Itram Khola. (C) Thick band of ferruginous metasandstone of the Melpani Formation at Nayagaun area. (D) Plant fossils (trunk and leaves) in mudstone at the Lower Siwalik at Mallakada area.

3.2 Structural features

3.2.1 Boudins

They are the structures formed by the stretching of the rock units. Due to extensional force in the active tectonic zone, certain layer of rock unit shows bulging and pinching structure. The boudinage structure is especially preserved in the pelitic rock units like phyllite in the Sisneri Formation and the Ranimatta Formation. The quartz veins formed in the foliated phyllite get deformed again to form the boudinage structures. These structures are seen through the whole sequence of the Sisneri Formation along with metabasic rocks and phyllite of the Ranimatta Formation (Figure 4(A)). The quartz vein indicated the extensional deformation after the first collisional deformation during which foliation and formation of the quartz vein occur. These types of asymmetric boudin are common shear sense indicators in ductile deformation zones.

3.2.2 Folds

The rocks in the Lesser Himalayan sequences (ie; Ranimatta Formation and Sisneri Formation) show a greater frequency of folding. The folds formed on sequences are subjected to episodic re-folding due to the continuous activity of tectonic stress resulting in the crenulated folds, formation of C-surface and formation of extensional features. The formation of several quartz veins and the foliation of host rock shows

evidence of D1 collisional phase and a D2 post collisional extension with the reactivation of some of the D1 structures occurring in the ductile-brittle transition resulting in the folding, thrusting, and formation of cracks and fractures within quartz veins itself (Figure 4(B)). Similarly, the rock of the Sisneri Formation and the Ranimatta Formation shows layer parallel shortening effect giving rise to the crenulated layers of folds (Figure 4(C)). Because of ductile deformation on the Dailekh Group rocks the frequency of the folds is more concentrated in the Ranimatta Formation and Sisneri Formation. Similarly, the rock of arenaceous origin shows the antiformal fold in the Melpani Formation (Figure 4(D)).

3.2.3 Faults

Regional thrusts giving rise to local faults and fractures have been widely distributed in the study area. The lithology varies along the thrust's regions based on the rock type of the underlying and overlying geological unit. The Thali Thrust is surrounded by the rocks of the Siwalik containing variegated mudstone and fine sandstone underneath it whereas carbonated rocks consisting of some layers of shale are presented over the thrust. Similarly, the Lade Thrust is surrounded by purple to greenish-gray shale and metasandstone beneath the thrust and greenish phyllite interbedded with white quartzite and some meta basics unit overlying it (Figure 5(A)). The overlying rocks of the Nigalpani Thrust include greenish highly deformed rocks consisting of psammitic phyllite with frequent quartz veins trusted over greenish gray.



Figure 4: (A) Boudinage structure seen in the green phyllite of the Ranimatta Formation indicating the ductile deformation. (B) Poly-deformed structure showing the quartz vein (D1 deformational structure) and refolding and formation of C-surface showing D2 deformation. (C) Folded quartzite layer in gray phyllite of the Ranimatta Formation (D) Antiformal fold in the metasandstone beds of the Melpani Formation near Sot Khola

phyllite dominated rocks. The Timile Thrust brings the gneissic rocks thrust over the deformed phyllites unit. The orientation of the local faults and the orientation of the C-surfaces show that they follow the major regional thrusts in the study area trending NW-SE direction. The presence of faults related to folds (Figure 5(B)), offset marker beds, conjugate faults, and secondarily filled fractures formed into two intersecting sets with

opposite shear sense resulted from the widespread activity of the faults in this area. The presence of offset of the marker beds (Figure 5(C)) and conjugate faults (Figure 5 (B)) in the Surkhet Group rocks shows the area is affected by the brittle deformation whereas conjugate folds, boudins, and C-surface indicates that the rocks of the Dailekh Group is affected by ductile deformation.

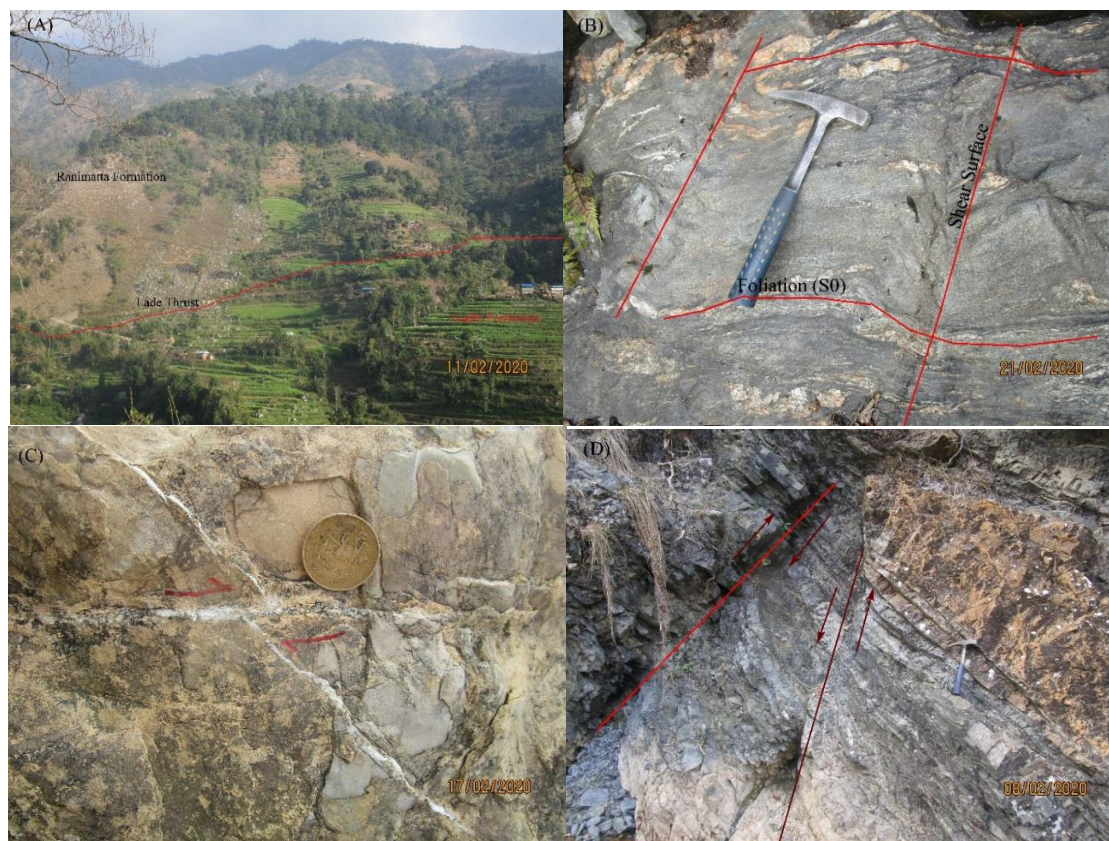


Figure 5: (A) Change in geomorphology in Tallo Ranimatta area because of Lade Thrust. (B) Formation of secondary fault plane shifting the folded quartz veins which indicates different phases of deformation. (C) Shifting of quartz vein due to faulting in shale of the Hattikhil Formation near Thali Village (D) Conjugate fault in the rocks of Melpani Formation.

3.3 Finite Strain analysis

To measure the finite strain caused by the regional and local tectonic stress in the study area, To measure the finite strain caused by the regional and local tectonic stress in the study area, seven oriented samples has been collected, and a thin section of each of the samples was prepared to

measure the long axis and short axis of the deformed quartz grains. The details of the samples used for the analysis are presented in Table 1. The extracted data from the quartz grain distribution in the thin section indicates the two different types of results based on the samples collected from two different tectonic zones: the Surkhet Group and the Dailekh Group.

Table 1: Details of samples subjected for finite strain analysis and vorticity analysis.

Sample	Formation	Rock type	Field Orientation	Mineral Assemblage	Strain markers
Surkhet Group					
A5	Melpani	Quartzite	315/32/45	Quartz \approx 90%, opaque \approx 8% and sericite \approx 2%	Small scale brittle faults
A16	Melpani	Metasandstone	286/76/16	Quartz \approx 80%, opaque \approx 17% and sericite \approx 3%	Fractured grains with filling of opaque minerals
C13	Gadhi	Green sandstone	320/43/50	Quartz \approx 65%, plagioclase \approx 20%, micas \approx 12% and matrix \approx 3%	
Dailekh Group					
J12	Ranimatta	Chlorite Schist	297/79/227	Quartz \approx 80%, sericite \approx 15% and opaque \approx 5%)	Boudinage structures
J19	Ranimatta	Metaquartzite	300/29/30	Quartz \approx 80%, sericite \approx 10%, chlorite \approx 7% and opaque \approx 3%)	Cross-cutting relation of quartz veins
L5	Sisneri	Quartzite	320/85/50	Quartz \approx 50%, muscovite \approx 19%, feldspar \approx 14%, chlorite \approx 11% and opaque \approx 6%	
M20	Sisneri	Psammatic phyllite	305/60/35	Quartz \approx 52%, sericite \approx 35% and feldspar \approx 13%.	Refolded quartz veins, forming of c-surface

3.3.1 Surkhet Group

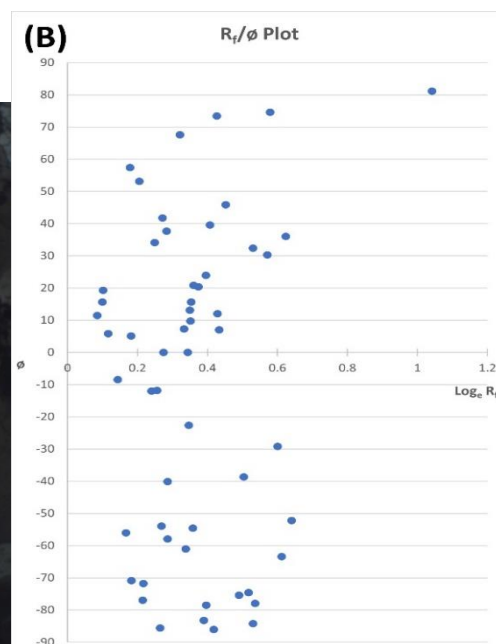
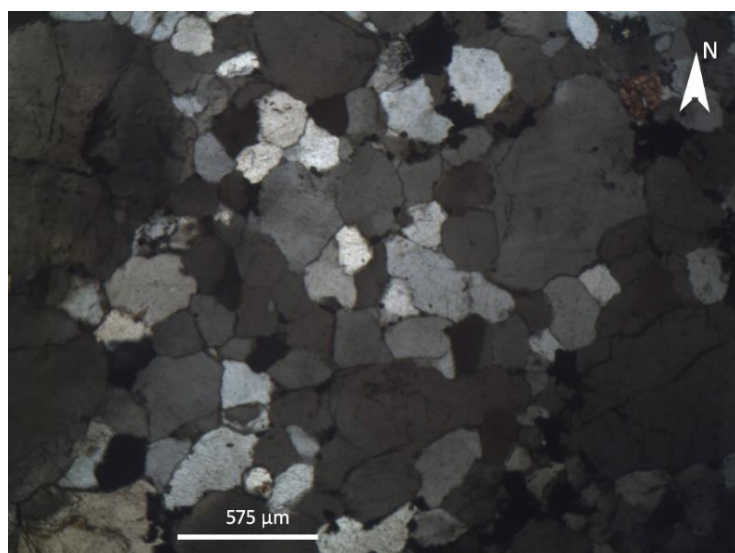
The R_f/ϕ graph plot shows that the quartz grains are distributed on the left part of the graph with the scattered point plot at a large area of the R_f/ϕ graph (Figure 6(B), 7(B), 8(B)). The long axis orientation plot in the frequency diagram (Figure 6(C), 7(C), 8(C)) gives the average orientation of the quartz grains after deformation with respect to the north. The maximum oriented data is concentrated at the angle of 0-10° for sample A5, 50-60° for sample A16, and -50--60° for sample C13 with respect to the north direction of the oriented samples.

The average long-axis orientation direction (ϕ) of each of the samples was calculated which was then plotted against the final ellipticity and then

contoured based on the Kernel Density plot in the R_f/ϕ graph to find out the maximum final strain ellipse ($R_{f\max}$) and the minimum final ellipse ($R_{f\min}$) along with the value of Fluctuation (F) (Table 2) (Figure 6(D), 7(D), 8(D)). The contours of the density data distribution indicated $R_i > R_s$ condition as ($F > 90^\circ$) for all the samples collected from the Surkhet Group rocks. Thus, the value of R_i and R_s for each of the samples A5, A12, and C13 is calculated using the equations illustrated in R_f/ϕ methods (Ramsay, 1967). The value of initial ellipticity (R_i) ranges from a maximum of 1.90 in sample C13 to a minimum of 1.47 in sample A16 whereas the value of strain Ellipse (R_s) ranges from the maximum value of 1.73 in sample C13 and a minimum value of 1.33 in sample A16 (Table 2).

Table 2: Finite strain data (R_s) for the rocks of Surkhet Group calculated using the R_f/ϕ method.

Sample	$R_{f\max}$	$R_{f\min}$	F	R_i	R_s	Remarks
A5	2.2255	1.1	163	1.564625	1.42238596	$R_i > R_s$
A16	2.18134	1.22	167	1.470871	1.337155042	$R_i > R_s$
C13	3.158	1.0512	135	1.906585	1.733258692	$R_i > R_s$



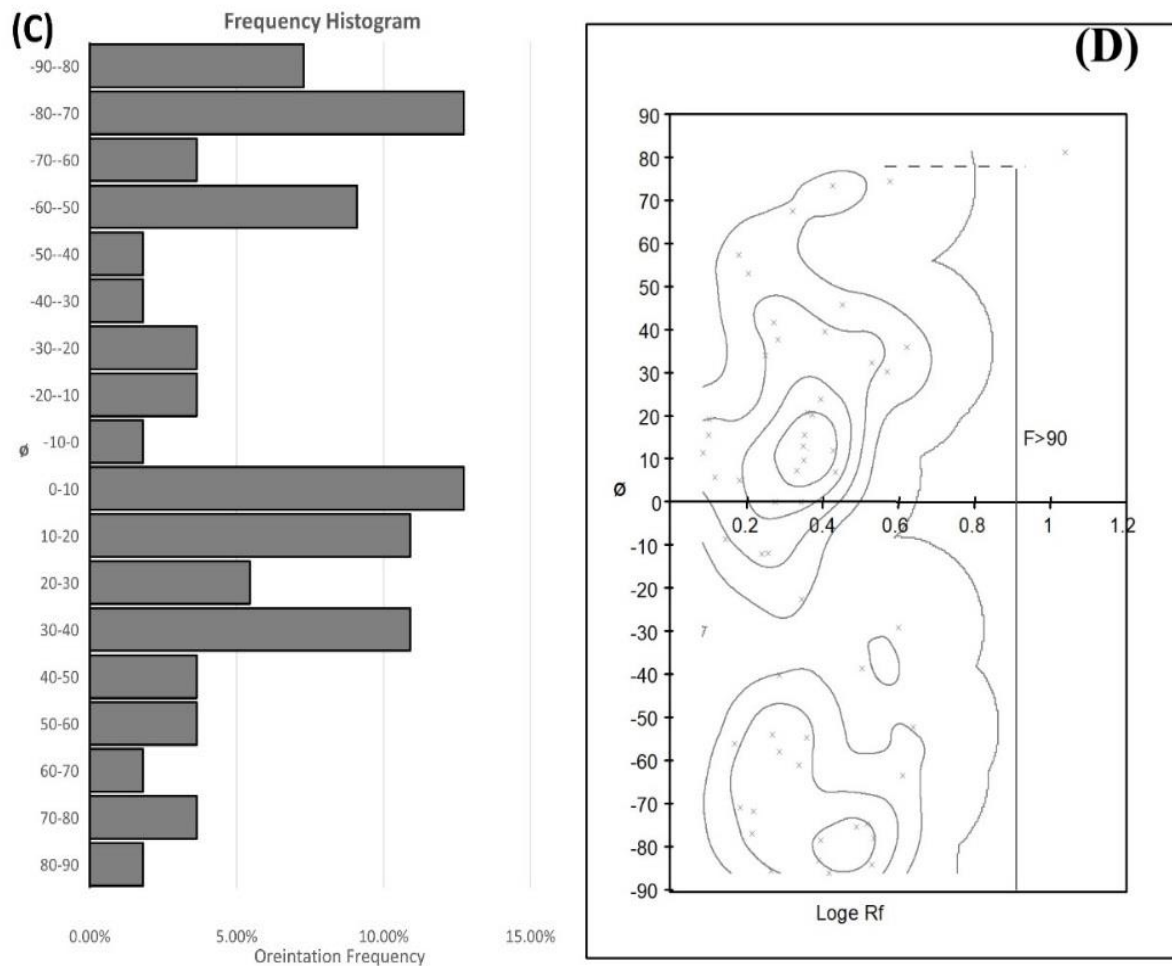
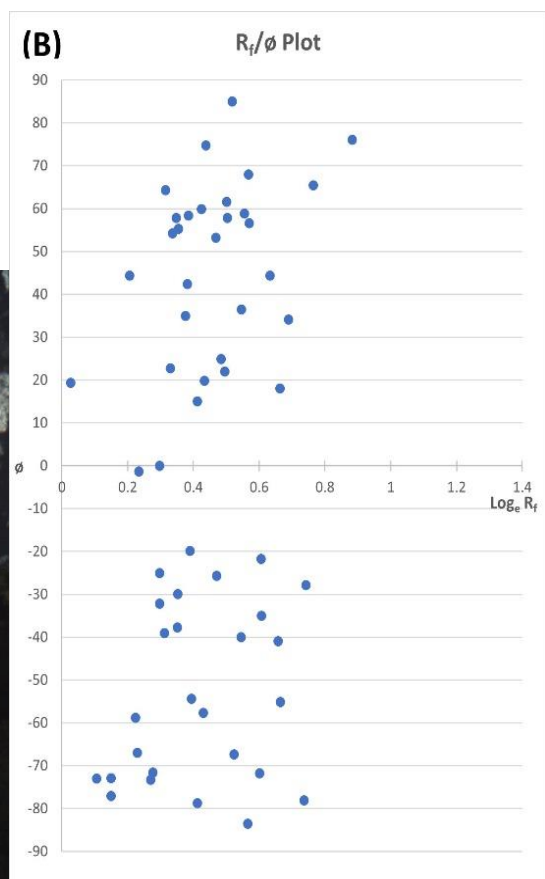
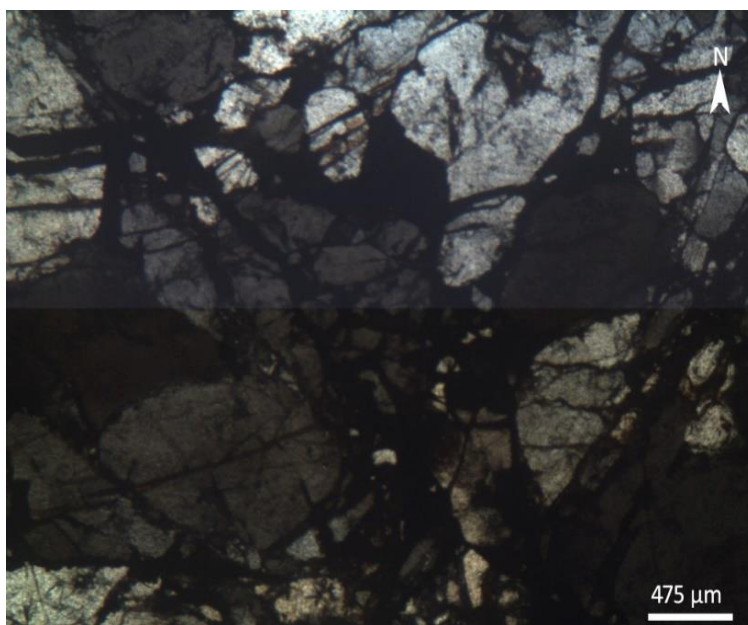


Figure 6: Analysis of sample A₅ (A) Photomicrograph showing the quartz grains (B) R_f/θ scattered plot of the data points (C) Histogram plot for analysis of the orientation frequency (D) Contour using Kernel Density plot for the scattered plot data. Where, R_f = Final ellipticity, θ = Angle made by long axis of quartz grains with respect to north, F = Fluctuation



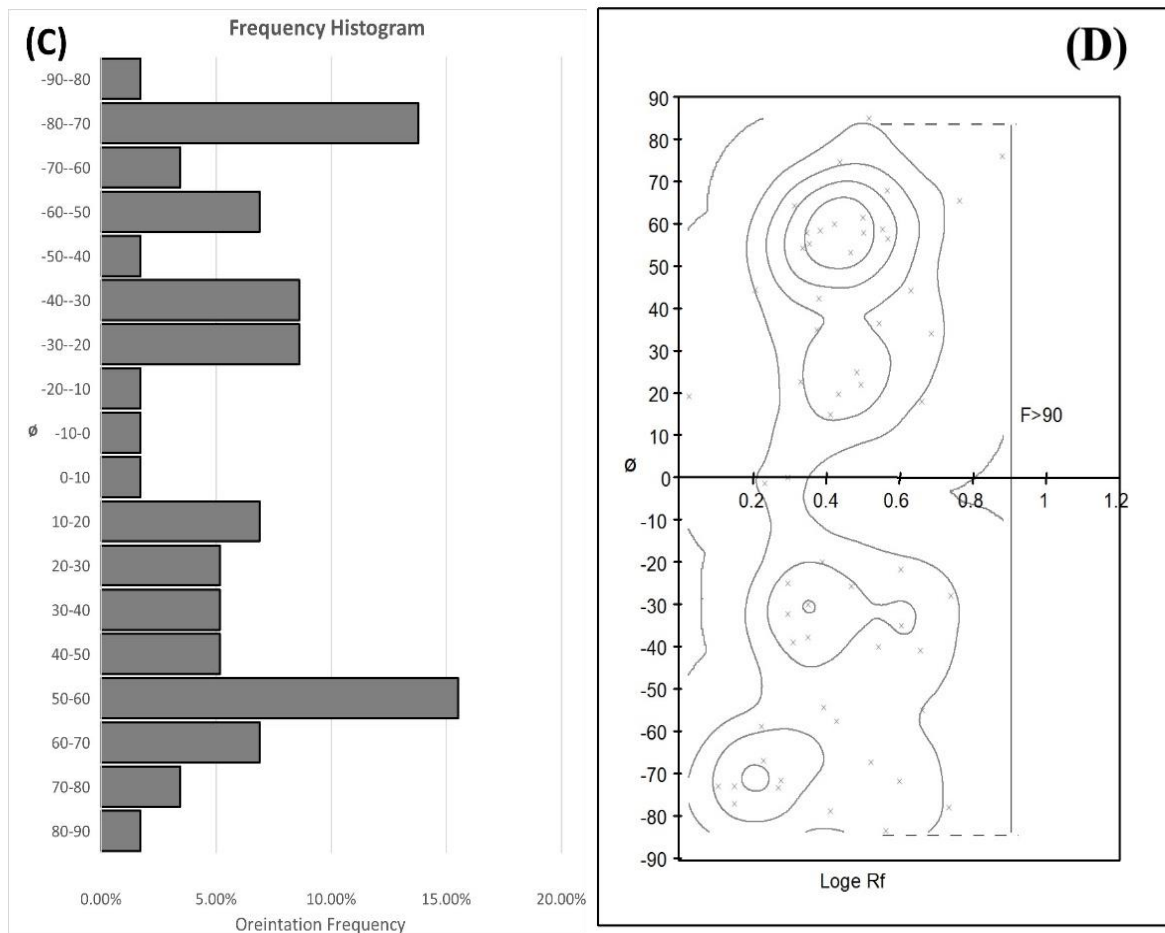
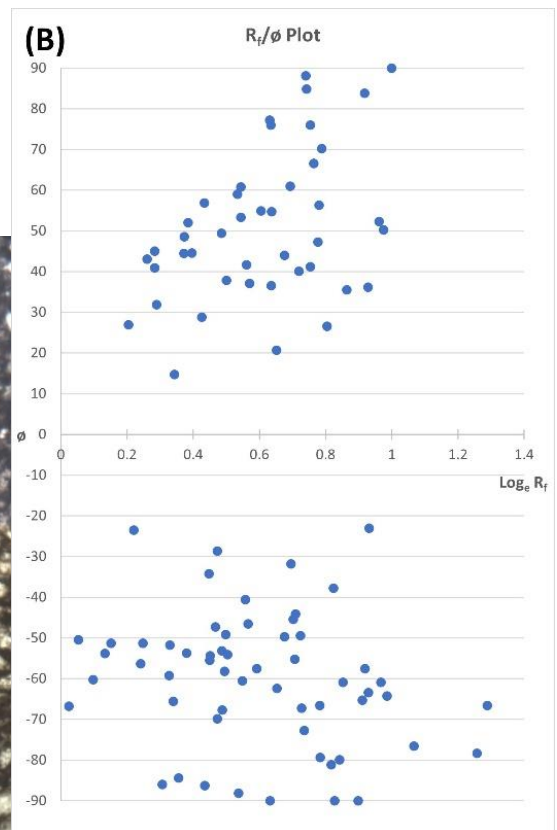
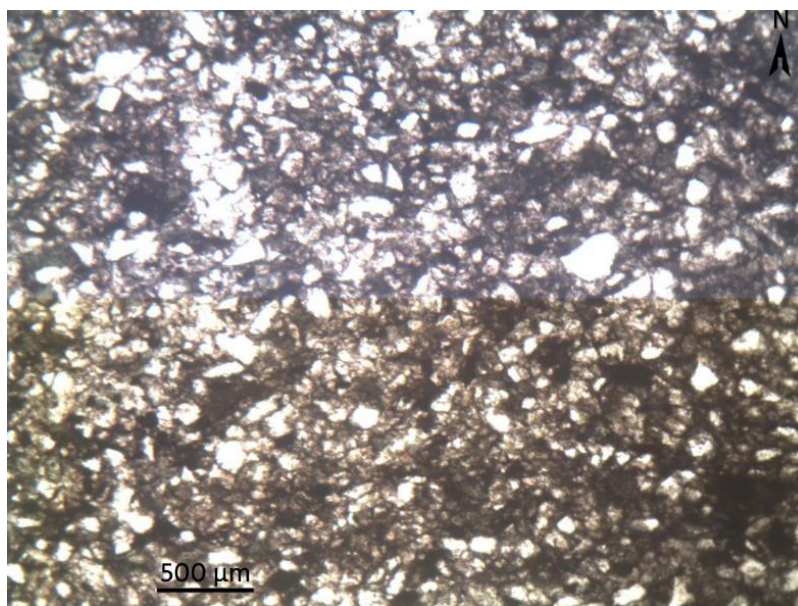


Figure 7: Analysis of sample A₁₆ (A) Photomicrograph showing the quartz grains (B) R_f/ϕ scattered plot of the data points (C) Histogram plot for analysis of the orientation frequency (D) Contour using Kernel Density plot for the scattered plot data. Where, R_f = Final ellipticity, ϕ = Angle made by long axis of quartz grains with respect to north, F = Fluctuation



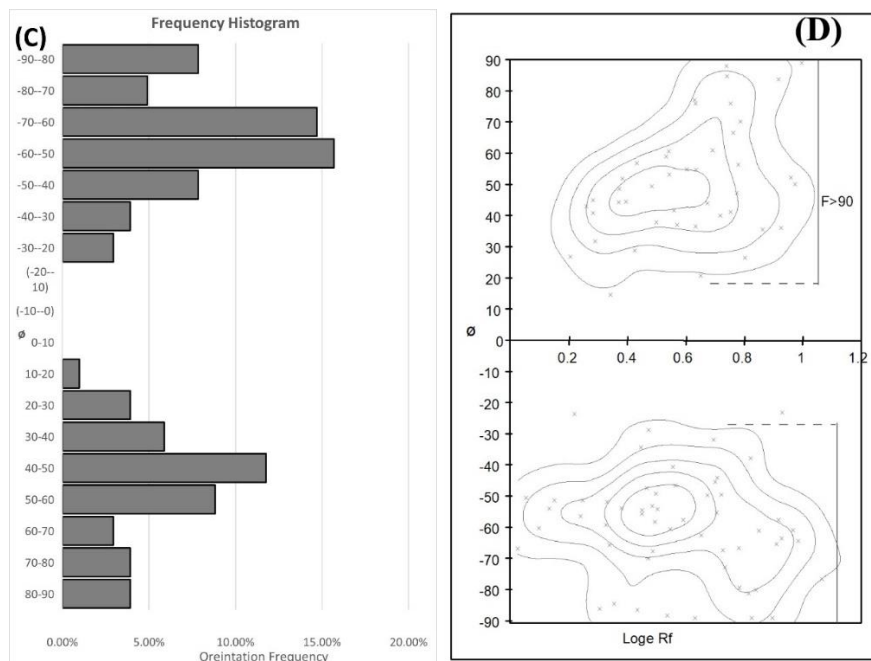


Figure 8: Analysis of sample C₁₃ (A) Photomicrograph showing the quartz grains (B) R_f/θ scattered plot of the data points (C) Histogram plot for analysis of the orientation frequency (D) Contour using Kernel Density plot for the scattered plot data. Where, R_f = Final ellipticity, θ = Angle made by long axis of quartz grains with respect to north, F = Fluctuation.

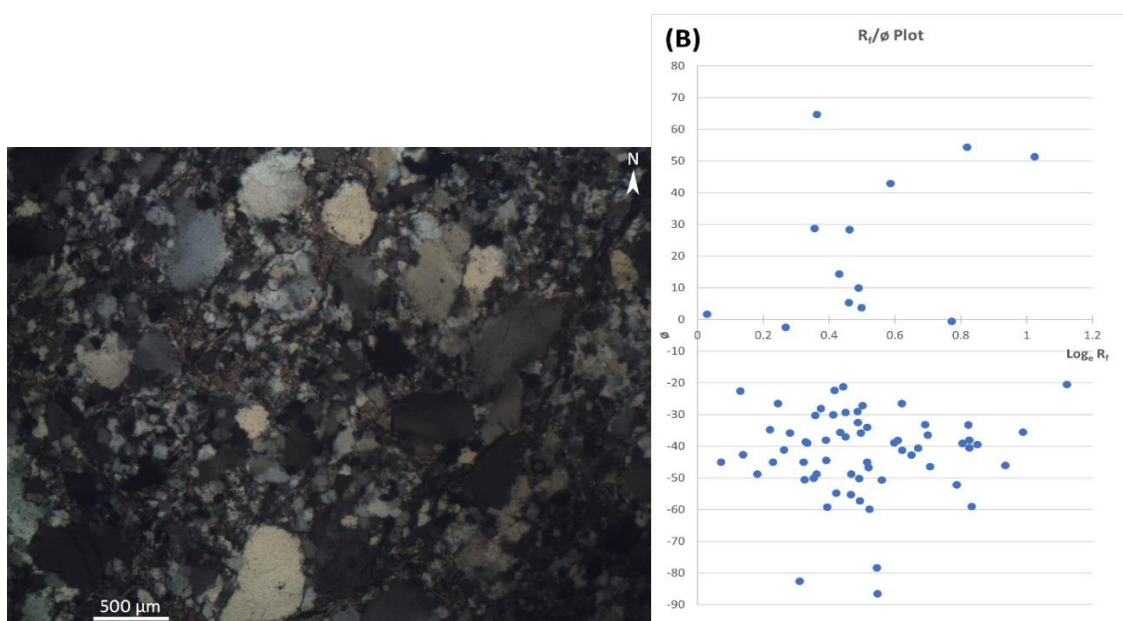
3.3.2 Dailekh Group

The R_f/θ graph plot shows the concentration of the plot in the restricted area of the scattered graph plotted (Figure 9(B), 10(B), 11(B), 12(B)). The maximum orientation frequency coincides with the long-axis orientation of the strain ellipse. The long axis orientation plot in the frequency diagram (Figure 9(C), 10(C), 11(C), 12(C)) gives the average orientation of the quartz grains after deformation with respect to the north. The distribution of the data points from the maximum orientation frequency is nearly symmetrical on both sides for all the samples of the Dailekh Group. The maximum orientation of the strain ellipse is concentrated at the angle of -35° – 40° for sample J12, 25° – 30° for sample J19, -35° – 40° for sample L5,

and an angle of 10° – 15° for sample M20. The R_f/θ scattered graph plot is then contoured based on the Kernel Density plot to find out the maximum final strain ellipse ($R_{f\max}$) and the minimum final ellipse ($R_{f\min}$) along with the value of Fluctuation (F) (Figure 9(D), 10(D), 11(D), 12(D)). The contours of the density data distribution indicated $R_i < R_s$ condition ($F < 90^{\circ}$) for all the samples collected from the Dailekh Group rocks (Table 3). Thus, the value of R_i and R_s for each of the samples J12, J19, L5, and M20 are calculated using the equations illustrated in R_f/θ methods (Ramsay, 1967). The value of initial ellipticity (R_i) ranges from a maximum of 1.60 in sample L5 to a minimum of 1.40 in sample J19 whereas the value of strain Ellipse (R_s) ranges from the maximum value of 1.86 in sample M20 and a minimum value of 1.69 in sample J12 (Table 3).

Table 3: Finite strain data (R_s) for the rocks of Dailekh Group calculated using the R_f/θ method.

Sample	R_i max	R_i min	F	R_i	R_s	Remarks
J12	2.5857	1.105	52	1.529706	1.690324969	$R_i < R_s$
J19	2.4596	1.246	60	1.40499	1.750617491	$R_i < R_s$
L5	2.8576	1.1051	65	1.608051	1.777057613	$R_i < R_s$
M20	2.787	1.246	50	1.495579	1.863491884	$R_i < R_s$



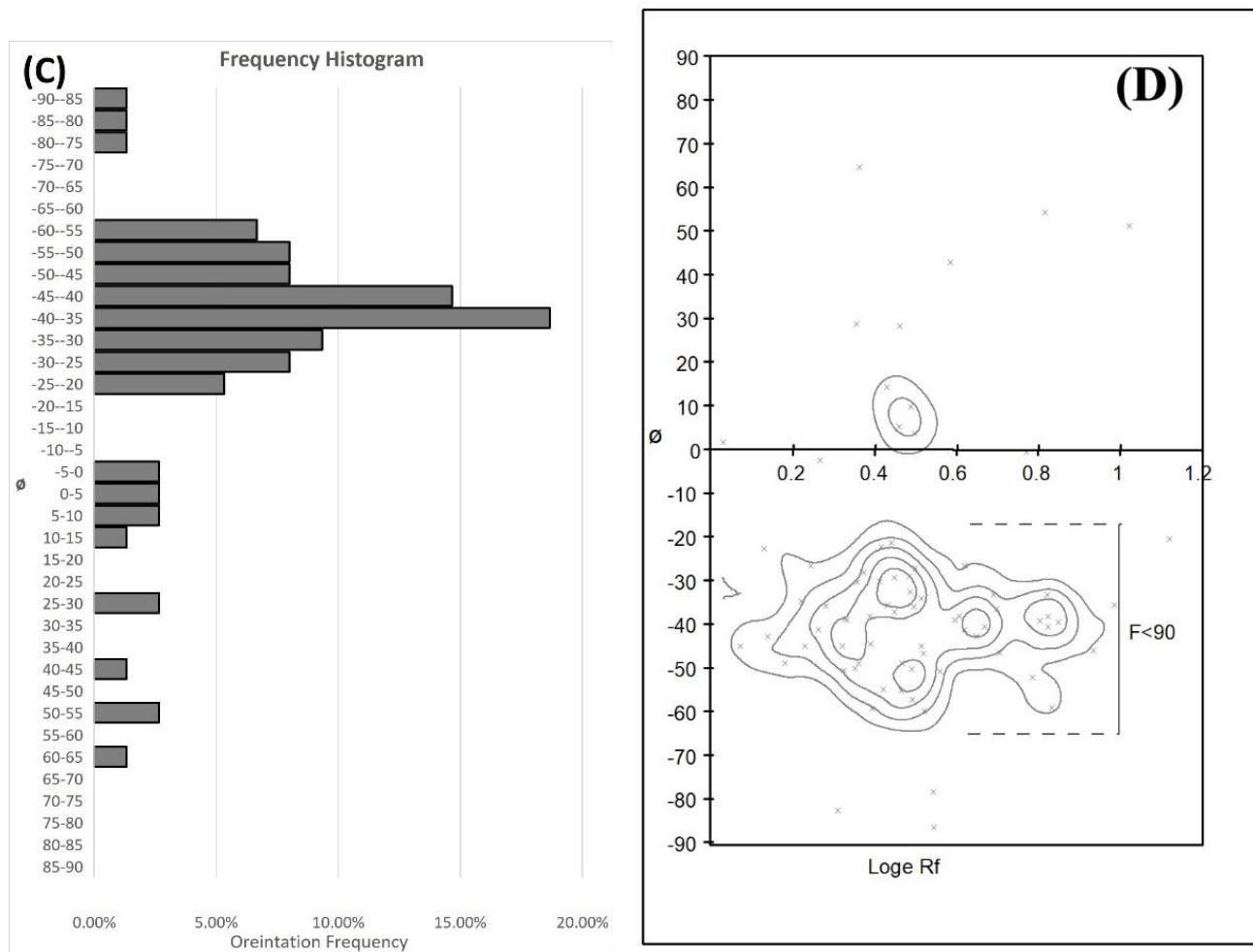
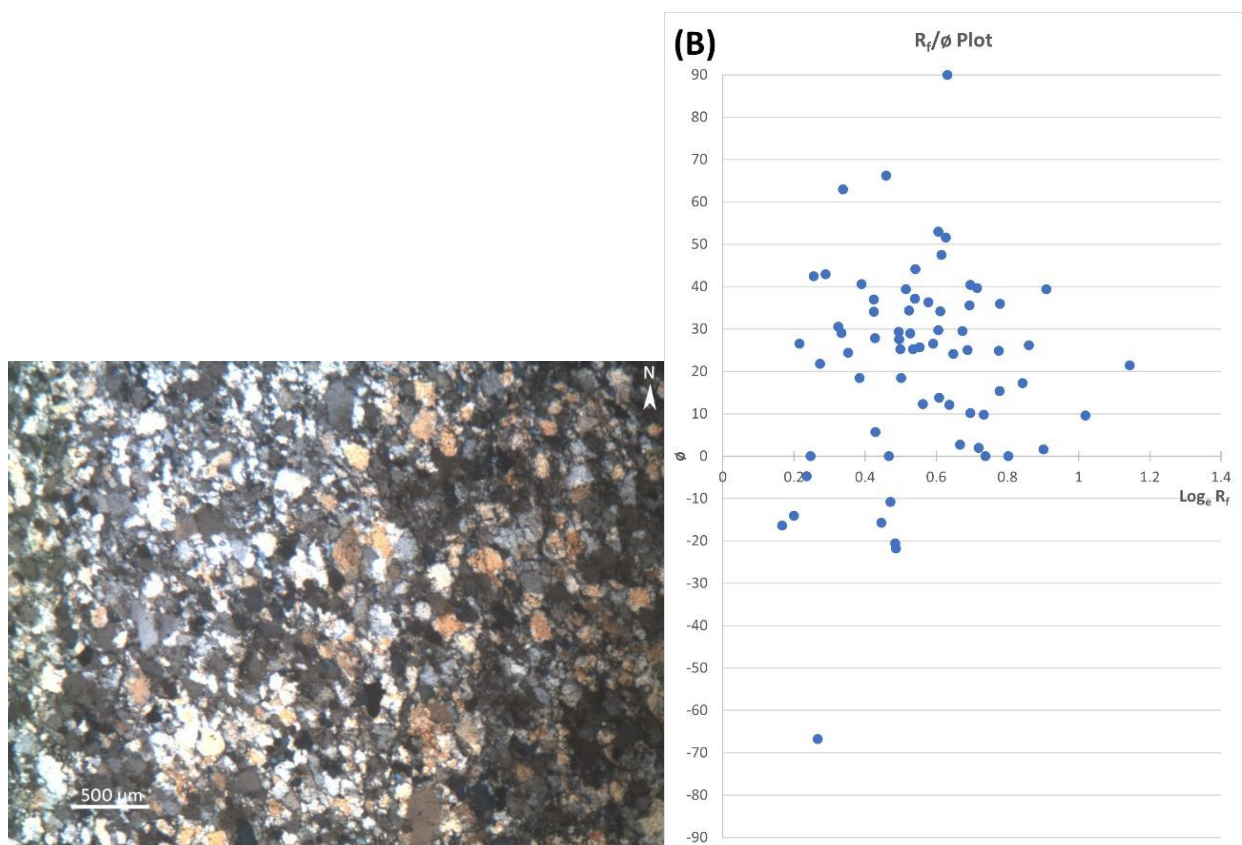


Figure 9: Analysis of sample J₁₂ (A) Photomicrograph showing the quartz grains (B) R_f/θ scattered plot of the data points (C) Histogram plot for analysis of the orientation frequency (D) Contour using Kernel Density plot for the scattered plot data. Where, R_f = Final ellipticity, θ = Angle made by long axis of quartz grains with respect to north, F = Fluctuation.



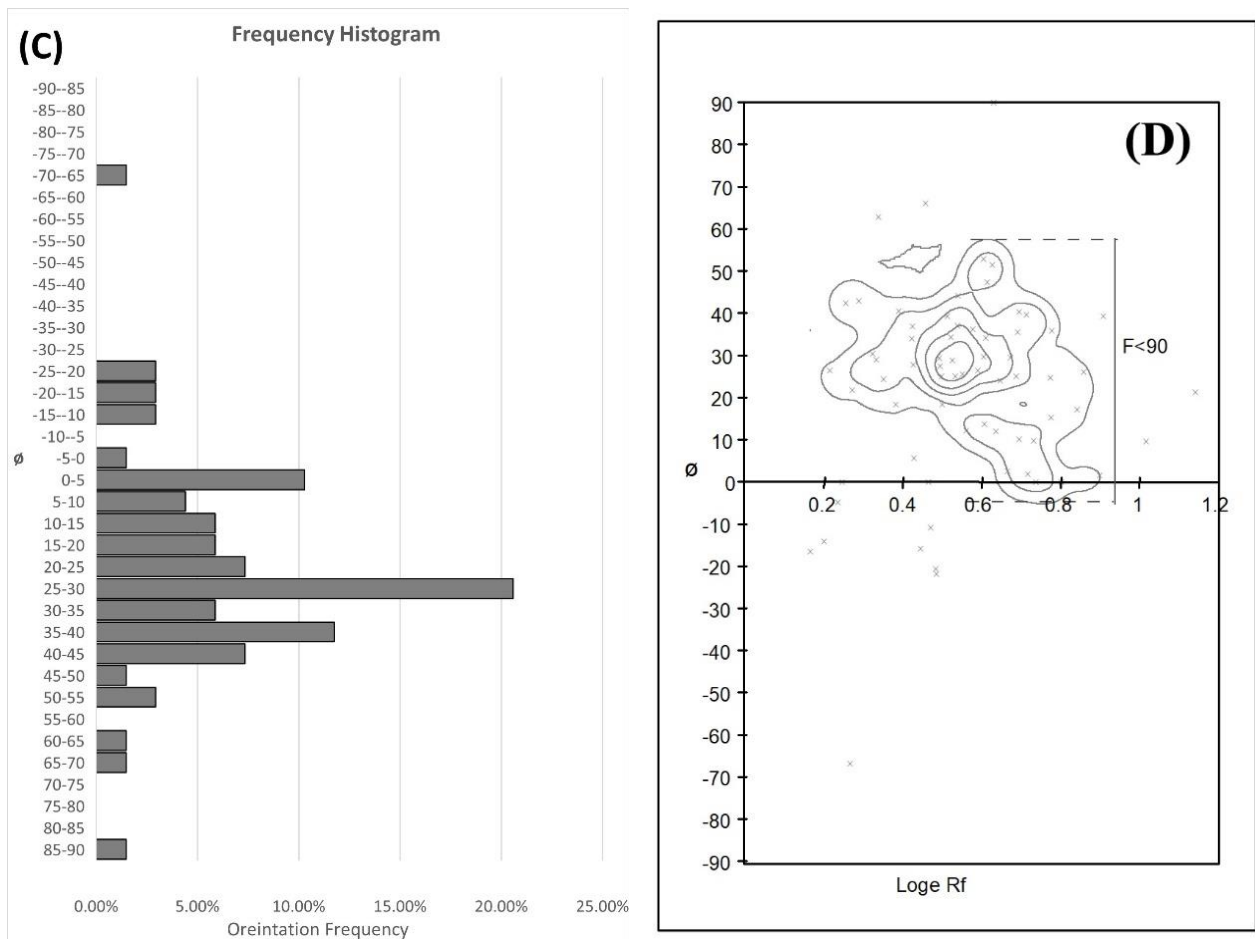
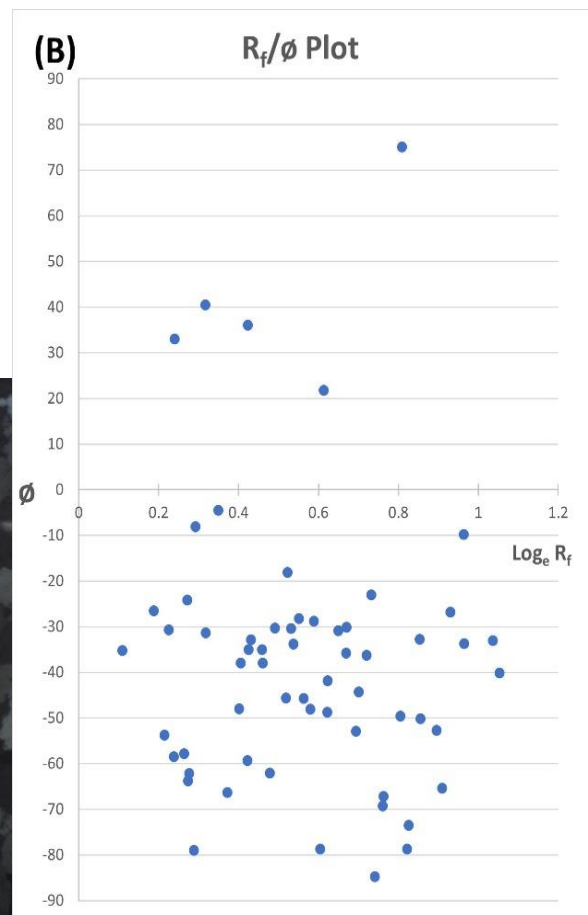
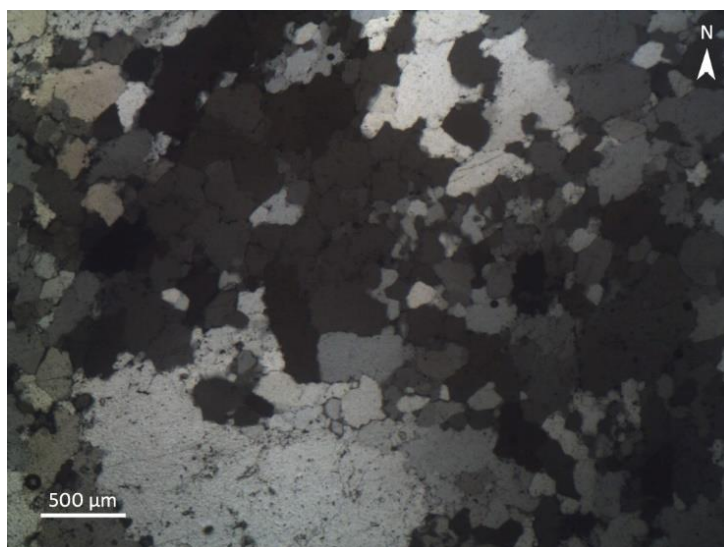


Figure 10: Analysis of sample J₁₉ (A) Photomicrograph showing the quartz grains (B) R_f/ϕ scattered plot of the data points (C) Histogram plot for analysis of the orientation frequency (D) Contour using Kernel Density plot for the scattered plot data. Where, R_f = Final ellipticity, ϕ = Angle made by long axis of quartz grains with respect to north, F = Fluctuation.



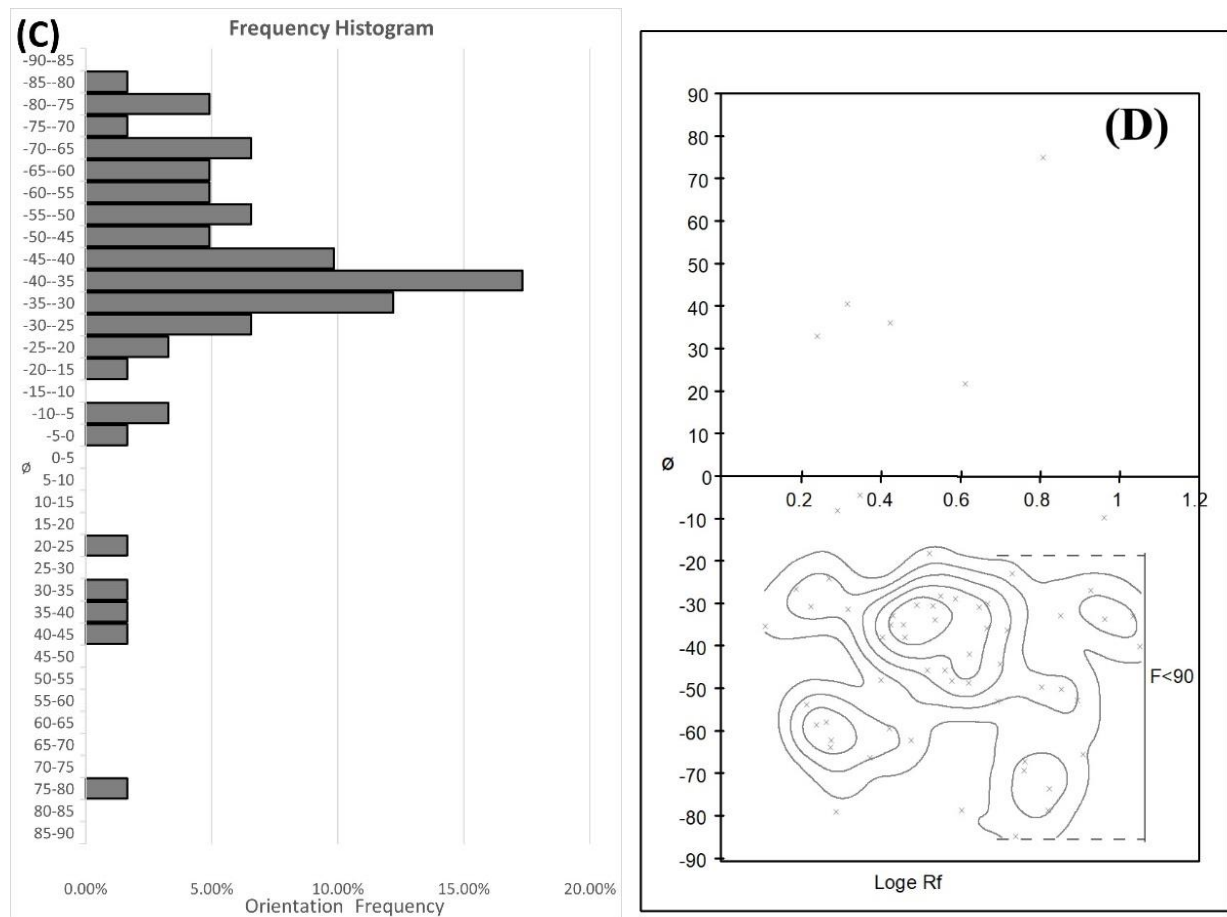
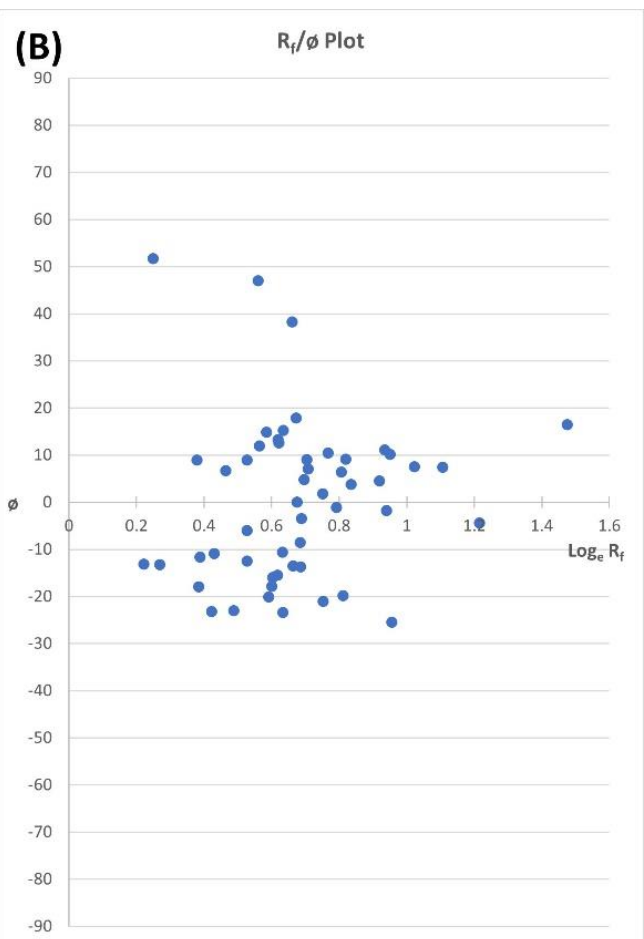
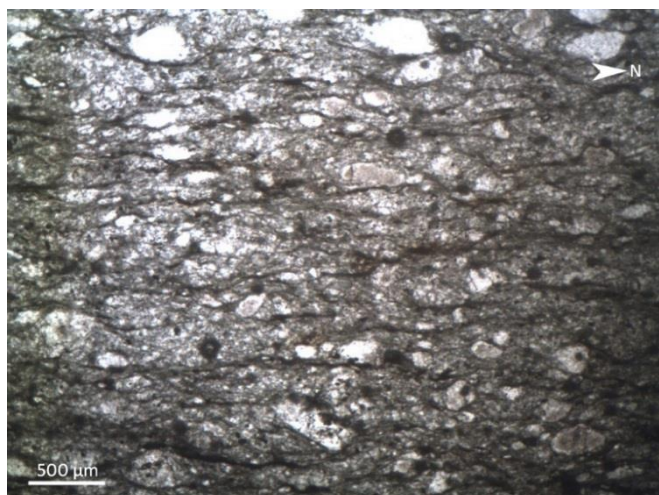


Figure 11: Analysis of sample L₅ (A) Photomicrograph showing the quartz grains (B) R_f/ϕ scattered plot of the data points (C) Histogram plot for analysis of the orientation frequency (D) Contour using Kernel Density plot for the scattered plot data. Where, R_f = Final ellipticity, ϕ = Angle made by long axis of quartz grains with respect to north, F = Fluctuation



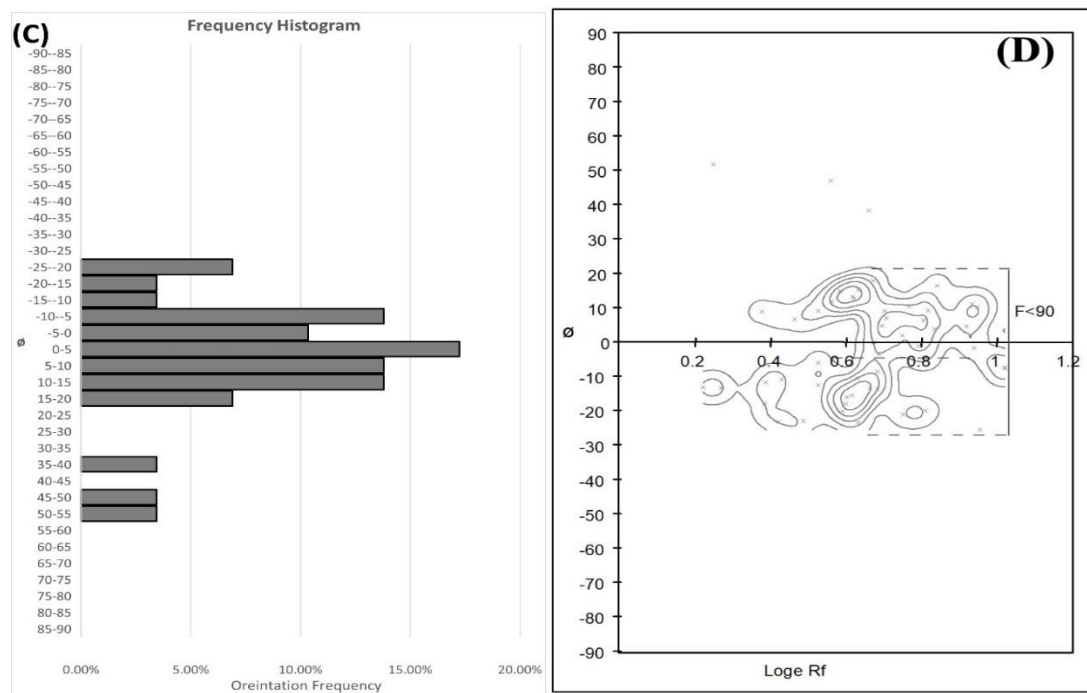


Figure 12: Analysis of sample M₂₀ (A) Photomicrograph showing the quartz grains (B) R_f/θ scattered plot of the data points (C) Histogram plot for analysis of the orientation frequency (D) Contour using Kernel Density plot for the scattered plot data. Where, R_f = Final ellipticity, θ = Angle made by long axis of quartz grains with respect to north, F = Fluctuation.

3.4 Vorticity Analysis

The kinematic vorticity number represents the non-linear ratio of pure shear ($W_m=0$) and simple shear ($W_m=1$) components of deformation (Means, 1994). Besides the several methods to study kinematic vorticity in the deformed rocks, all of these used the average value of vorticity (W_m) (Xypolias, 2010; Passchier and Trouw, 2005; Xypolias, 2010). Thin section prepared from the different samples of the Dailekh Group only are subjected to the analysis of kinematic vorticity (W_m) because the shear band surface (C-surface) and the angle made by the long axis of the grains

with this surface are clearly seen from these samples, whereas the samples collected from the Surkhet Group rocks shows greater deflection in the orientation of the grains without the development of shear band surface (C-surface) due to the less amount of strain ellipsoid (R_s) applied over these rock units than its initial ellipticity (R_i). All the available methods of vorticity analysis are based on analytical models of homogeneous steady-state flows and are limited to assumptions. Some of the complex factors can influence the accuracy of the estimate, which is difficult to assess (Xypolias, 2010).

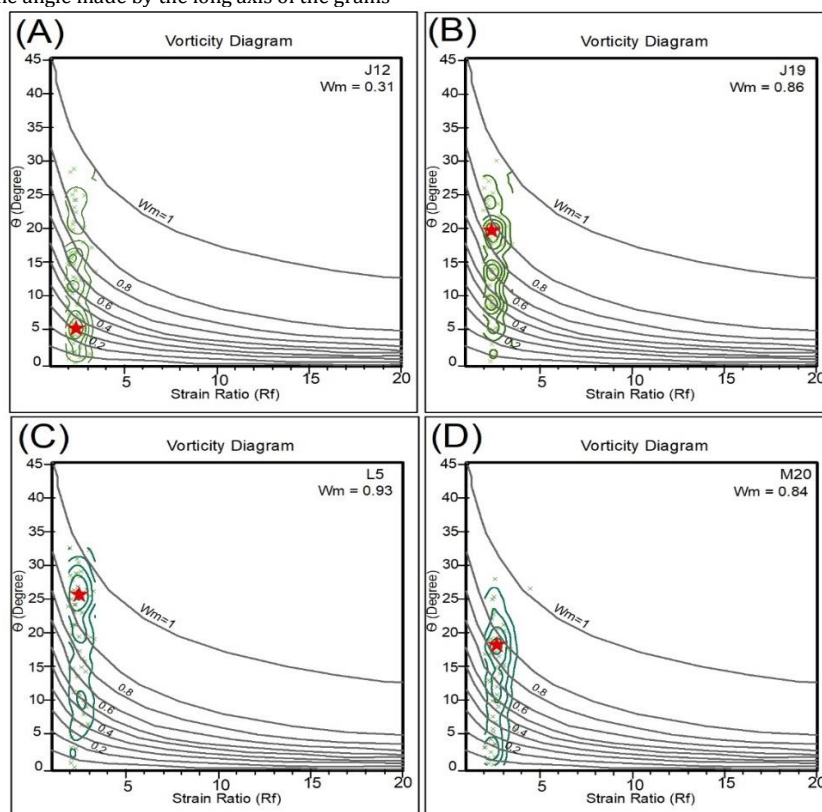


Figure 13: Nomogram of finite strain ratio R_f vs. angle θ for various kinematic vorticity numbers (W_m) values (A) Nomogram for sample J12. (B) Nomogram for sample J19 (C) Nomogram for sample L5. (D) Nomogram for sample M20 (After Tikoff and Fossen 1995). Green cross sign denotes value of each grain, green line denotes contours drawn based on kernel density plot and red star denoted the maximum concentrated values which is considered to find the value of vorticity number (W_m).

The angle of deflection of the quartz grain's long axis with the C-surface is plotted against the final ellipticity (R_f) of each of the grains and then contoured based on the kernel density plot to find out the maximum concentration of the orientated grains. The maximum concentration point is then considered to find out the vorticity number (W_m). Among the four

samples (J12, J19, L5, and M20), sample L5 has the greatest value of vorticity ($W_m = 0.93$) whereas the lowest value of the vorticity ($W_m = 0.31$) is obtained from sample J12 (Figure 13 (A, C)). Similarly, the vorticity number (W_m) of 0.86 and 0.84 are obtained from the nomogram (R_f - θ) plot of samples J19 and M20 respectively (Figure 13 (B, D)).

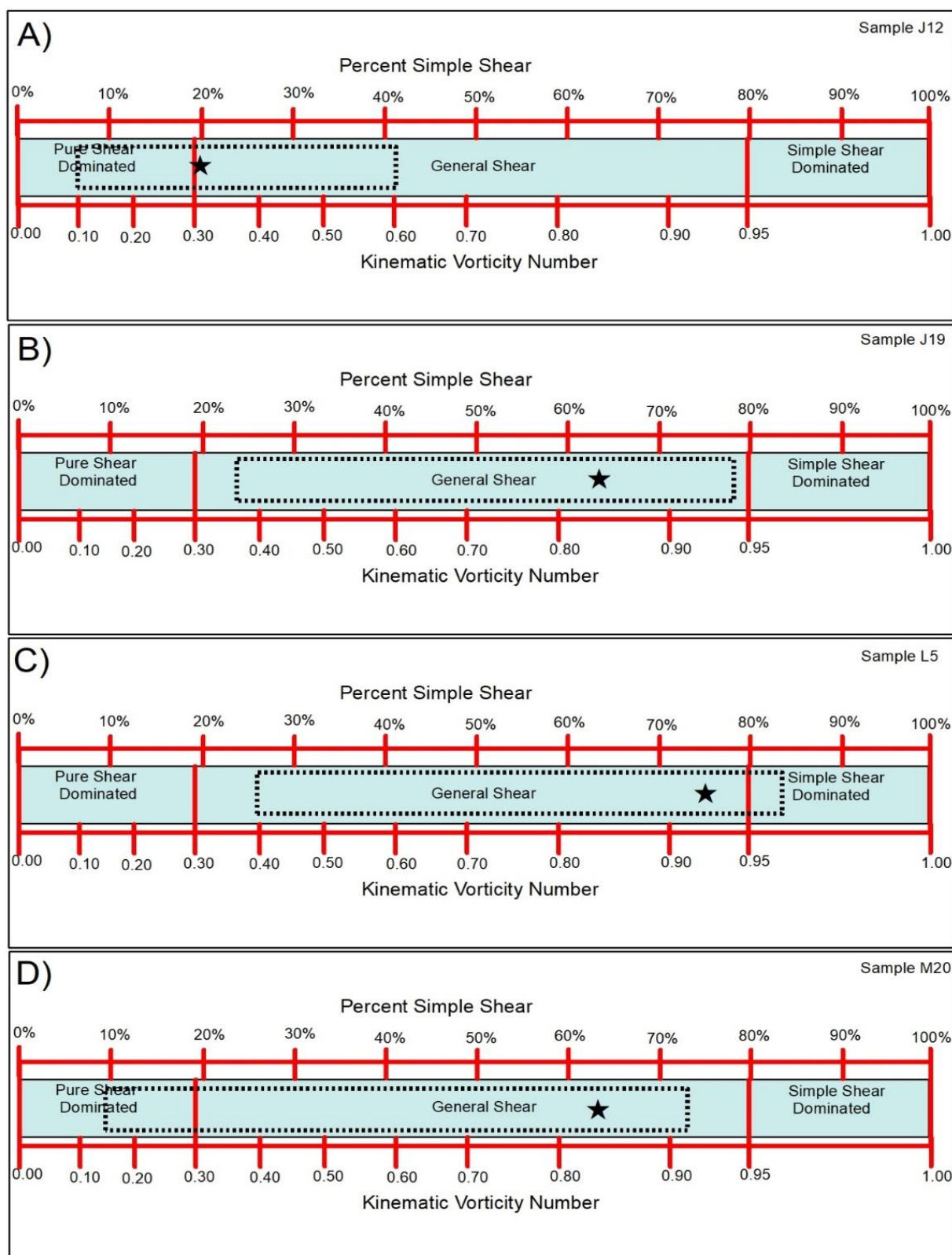


Figure 14: Relationship between Kinematic vorticity number (W_m) and components of pure shear and simple shear (Redrawn from (Forte and Bailey, 2007). (A) Analysis for sample J12, (B) Analysis for sample J19 (C) Analysis for sample L5 (D) Analysis for sample M20. (Black dot box denotes range of data distribution and black star denotes value of maximum concentrated data).

Based on the applied vorticity method the measured kinematic vorticity number of the rocks in the Dailekh Group ranges from $W_m = 0.31$ to 0.93 which confirms the general shear deformation condition. The relation between the kinematic vorticity number and component of pure and simple shear shows the deviation from both simple shear (20%-75%) and

(25%-80%) pure shear indicated that the rock was subjected to the differential effect of shearing depending on the distance of the shear zone (Forte and Bailey, 2007). The sample J12 shows 21% simple shear whereas samples J19, L5 and M20 shows 63%, 75% and 62% simple shear respectively (Figure 14). The higher value of the kinematic vorticity

numbers ($W_m = 0.93$ for sample L5, $W_m = 0.86$ for sample J19 and $W_m = 0.84$ for sample M20) are located near to the thrust faults (Figure 14(B, C, D)). Sample J19 lies near the Timile Thrust whereas samples L5 and M20 lie near the Nigalpani Thrust. The sample J12 with the vorticity number $W_m = 0.31$ lies at some distance from any thrust.

4. DISCUSSIONS

The Birendranagar-Talpokhari section of the study area represents major parts of the Lesser Himalaya with some Sub Himalayan sequence. The Precambrian to early Miocene Lesser Himalaya sequence is divided into seven stratigraphic units, whereas the Sub Himalaya (Siwalik) unit consists of the Lower Siwalik rocks only. Many researchers have studied the regional geology of the region and described the stratigraphy of the region. Fuchs provides the outline of the geology of Karnali and Dolpo region on which his attempt is focused on the correlation of the

lithostratigraphy with the western Himalaya; Kumaon region established by (Fuchs and Frank, 1970). Later in 1977, he established the geology of Karnali and Dolpo region representing the major units as; Siwalik, Tansing unit, and Chail Nappe. Similarly, a group researcher have revealed this region consists of the sedimentary rocks of the Siwalik, low-grade metamorphosed rocks of Gondwanas, Midland Calcareous Group and Midland Aeraneous Group (Hayashi et al., 1984). Dhital has collected all the information and established the stratigraphy of the region (Dhital, 2015). He divided the rock units of this region into three groups: Surkhet Group, Lakharpata Group and Dailekh Group. Instead of all the established stratigraphy of the region the lithological unit consists of some variation in the lithological content, its extension, the dominance of rock type, and the type locality of the major exposure of each rock unit. Based on these parameters an attempt has been made to establish the stratigraphical units based on the local naming. These units can be correlated with the regional stratigraphy established by different authors as shown (Table 4).

Table 4: Correlation of lithostratigraphy with adjacent region.

Fuchs (1977)		Hayashi et al. (1984)	Dhital (2015)		DMG (1987)		Present Study	
Siwalik	Siwalik	Siwaliks	Siwalik	Lower Siwalik	Siwalik	Lower Siwalik	Siwalik	Lower Siwalik
Tansing Unit	Dagshai Formation	Gondwanas	Surkhet Group	Suntar Formation	Surkhet Group	Suntar Formation	Surkhet Group	Gadhi Formation
	Subathu Formation			Swat Formation		Swat Formation		Sotkhola Formation
	Tal Formation			Melpani Formation		Melpani Formation		Melpani Formation
	Korl Formation	Midland Calcareous Group	Lakharpata Group		Lakharpata Group	Gwar Formation	Lakharpata Group	Hattikhil Formation
Chail Nappe	Nagthat Formation	Midland Arenaceous Group	Dailekh Group	Ranimatta Formation	Dubhidanda Formation	Dailekh Group	Dailekh Group	Ranimatta Formation
	Phyllitic Unit	MCT Group		Green Phyllite and Metasandstone				Sisneri Formation
	Metagranite or Gneisses	Himalayan Group		Mylonitic Gneiss				Talpokhari Gneiss

Since, the area is highly affected by the tectonic activity there are many different structures separating and replacing the one litho-unit to another. The indication of these thrusts was studied in the area can also be correlated with the work of Dhital as shown (Table 5) (Dhital, 2015).

Table 5: Correlation of thrusts present in study area with Dhital.

Thrusts in study area	Dhital (2015)
Timile Thrust	Lohore Thrust
Nigalpani Thrust	Parajul Thrust
Lade Thrust	Budar Thrust
Thali Thrust	Jarbuta Thrust

Examining strain ellipsoid of the quartz grains from the study area shows that the rocks of Surkhet Group and Dailekh Group bear a differential deformation pattern. All the samples from the Surkhet group rocks show the greater scatteredness of the orientation with respect to the north direction in the R_i/ϕ plot. This shows the initial ellipticity (R_i) exceeds the strain ellipsoid (R_s). As the initial ellipticity is dominant over the strain ellipsoid, the rocks of the Surkhet Group bear a low amount of stress condition. Since this condition is verified in the field observation as the rocks are slightly metamorphosed and fossil remains are well preserved within the rock units without significant destruction due to the brittle deformation.

Similarly, the rock of Dailekh Group shows the concentrated orientation within the restricted area of the R_i/ϕ plot so that the initial random orientation of the quartz grains gets highly affected by the deformation caused by the regional deformation and by the deformation due to the effect of thrusts. Since the orientation of the long axis of the quartz grains are parallel to sub-parallel to the foliation of the rocks, it is because in response to the tectonic shearing of the area. The fluctuation of the orientation of the long axis limited below 90° indicates the strain ellipsoid is dominant over the initial ellipticity ($R_s > R_i$) of the grains. This condition proves that the rocks are subjected to high-stress deformation. Field verification of the exposure and samples also shows that the rocks of the

Dailekh Group are highly deformed with well-developed foliation and other deformation structures. The abundance of macroscopic deformation structures like asymmetric fold, boudinage, and oblique stretching lineation indicates that the unit is subjected to the oblique tectonic shifting towards the south.

The measurement of the quartz grain ellipticity was done assuming that the measured ellipticity approximates fine-strain ellipsoids. By only analyzing the quartz grains any strain components that can accommodate and hide some amount of simple shear deformation cannot be accounted (Mookerjee et al., 2016). As dynamic recrystallization is a process of crystal regrowth under conditions of stress and elevated temperature and the quartz having a relatively lower melting point undergoes the melting and recrystallization process. The thin section study of the quartzite from the upper part of the Ranimatta Formation near the Nigalpani Thrust shows frequent Bulging Recrystallization and few Subgrain Rotation Recrystallization (Figure 11(A)). This process of recrystallization may lose the integrity of strain markers in some grains so that the grains that undergo the recrystallization process are omitted to measure the strain ellipsoid.

Based on the applied vorticity method the measured kinematic vorticity number of the rocks in the Dailekh Group ranges from $W_m = 0.31$ to 0.93 which confirms the general shear deformation condition. The deviation from both simple shear (20%-75%) and (25%-80%) pure shear indicated that the rock was subjected to the differential effect of shearing depending on the distance of the shear zone. The higher value of the kinematic vorticity numbers (sample J19, L5, and M20) is located near the thrust faults whereas the sample with a low kinematic vorticity number (sample J19) lies at some distance from any thrust (Figure 15(A)). The vorticity analysis of all the samples shows that its value decreases systematically towards the middle part of the thrust sheet (i.e.: on going to the distance from the thrust fault). The vorticity number and their corresponding relation with the components of pure and simple shear shows that samples near to the thrust shows the greater component of the simple shear whereas on the greater distance from the thrust the simple shear component gradually decreases resulting in the dominance of the pure shear component (Figure 15(B)).

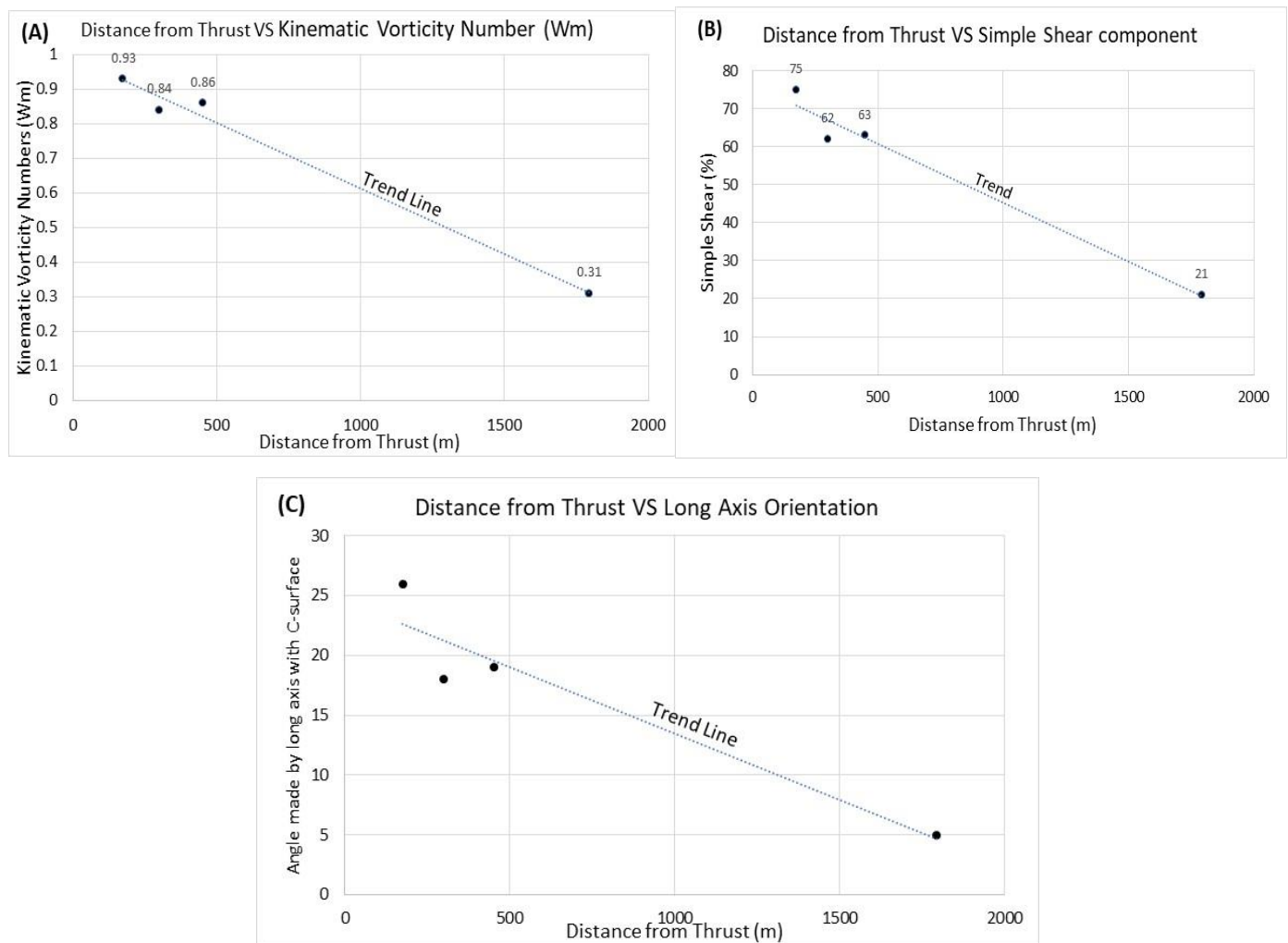


Figure 15: Relation of deformation with respect to the distance from the thrusts. (A) Kinematic vorticity number (W_m) VS Distance from nearest thrust. (B) Simple Shear component VS distance from the nearest thrust. (C) Angle made by long axis orientation (θ) with respect to C-surface VS Distance from the Nearest Thrust.

The simple shear-dominated area is more affected by the shearing effect near the thrust surface so that the long axis of the quartz grains gets affected and subjected to rotation during shearing making the higher angle with respect to the C-surface on going near to the thrust (Figure 15(C)). This result supports the presence of the regional thrusts; (Timile thrust and Nigalpani thrust) differentiating the Talpokhari Gneiss with Sisneri Formation and Sisneri Formation with Ranimatta Formation respectively. Similarly, the results also support that the Dailekh Group rock is an Allochthonous unit since the pure shear component of the fault zone has caused thinning associated with modest displacement relative to overall strain and the simple shear component caused displacement along the shear zone with little shortening/ thinning across the shear zone (Fuchs, 1974; Samani et al., 2019). The deformational shear sense indicators such as boudinage, oblique stretching lineation, and asymmetrical folds also indicate the regional shifting of the Dailekh Group rocks towards the south resulting in the ductile deformation of rock units.

The vorticity number for the rocks of the Surkhet Group cannot be determined since the rocks are subjected to low metamorphic condition resulting in minimal deformation. Similarly, the shear band surface (C-Surface) is absent on the rock samples so that fluctuation of the quartz grain long axis to the shear band surface cannot be determined.

5. CONCLUSIONS

Birendranagar-Talpokhari section of present study area represents a part of Lesser Himalaya and Sub Himalaya sequence. The Sub Himalayan unit consists of rocks of Lower Siwalik. This unit is characterized by the presence of fine-to-medium-grained light grey to grey sandstones with lamina intercalated with variegated reddish yellow to pale yellow mudstones. The Lesser Himalayan sequence consists of three tectonic units as: the Dailekh Group, Lakharpata Group and Surkhet Group. The Surkhet Group is the Para-autochthonous rock unit consisting of normal sequences of low-grade metamorphic rocks with some fossiliferous horizons whereas the Lakharpata Group consists of the dominance of

carbonate rocks. The Dailekh Group is an allochthonous rock unit consisting of sequences of different metamorphosed rocks like phyllite, quartzite, metasandstone, and metabasic rocks. This Group is thrust over the para-autochthonous rock units of the Surkhet Group.

Investigation of the strain pattern of deformed quartz grains from the study area shows that the rocks of the Surkhet Group and the Dailekh Group bear the differential pattern of deformation in response to the tectonic stress. All the samples from the Surkhet Group rocks show $R_i > R_s$ condition. As the initial ellipticity is dominant over the strain ellipsoid, the rocks of the Surkhet Group bear a low amount of stress condition. Similarly, the rock of Dailekh Group shows a concentrated orientation, so the rocks are highly affected by the tectonic condition. The fluctuation of the orientation of the long axis limited below 90° indicates the strain ellipsoid is dominant over the initial ellipticity ($R_s > R_i$) of the grains. This condition proves that the rocks are subjected to high-stress deformation.

Based on the applied vorticity method the measured kinematic vorticity number of the rocks in the Dailekh Group ranges from $W_m = 0.31$ to 0.93 which confirms the general shear deformation condition. The deviation from both simple shear (20%-75%) and (25%-80%) pure shear indicated that the rock was subjected to the differential effect of shearing depending on the distance of the shear zone. The higher value of the kinematic vorticity number is located near the thrust faults. The samples near to the thrust show a greater percentage of the simple shear whereas, at a greater distance from the thrust, the simple shear component gradually decreases resulting in the dominance of the pure shear component. This result supports the presence of the regional thrusts; (Timile Thrust and Nigalpani Thrust). Similarly, the results also support that the Dailekh Group rock is an allochthonous unit.

ACKNOWLEDGEMENT

First author is grateful towards the partial research grant from the Nepal Geological Society. Authors are grateful towards Prof. Rodolfo Carosi for

his suggestions while preparing the first draft of the manuscript. We extend our sincere acknowledgment to the Central Department of Geology for the laboratory facilities to prepare the thin sections.

REFERENCES

- Bilham, R., Larson, K., Freymueller, J., 1997. GPS measurements of present-day convergence across the Nepal Himalaya. *Nature*, 386, Pp. 61-64.
- Dhital, M.R., 2015. Lesser Himalaya of Mahakali-Seti Region. In *Geology of the Nepal Himalaya*. Springer. pp. 81-91.
- Dhital, M.R., Kizaki, K., 1987. Structural aspect of the northern Dang, Lesser Himalaya. *Bulletin of the College of Science, University of Ryukyus, Okinawa*, 45, Pp. 159-182.
- Forte, A.M., Bailey, C.M., 2007. Testing the Utility of the Porphyroclast Hyperbolic Distribution Method of Kinematic Vorticity Analysis. *Journal of Structural Geology*, 29 (6), Pp. 983-1001.
- Fuchs, G., 1974. On the geology of the Karnali and Dolpo regions, west Nepal. *Mitteilungen der Geologischen Gesellschaft in Wien*, 66 (67), Pp. 21-35.
- Fuchs, G., 1977. The geology of the Karnali and Dolpo regions, western Nepal. *Jahrbuch der Geologischen Bundesanstalt*, Pp. 165-217.
- Gansser, A., 1964. *Geology of the Himalayas*. New York: Wiley InterScience.
- Hayashi, D., Fujii, Y., Yoneshiro, T., Kizaki, K., 1984. Observations on the geology of the Karnali region west Nepal. *Journal of Nepal Geological Society*, v. 4, Pp. 29-40.
- Le Fort, P., 1975. Himalayas: the collided range. Present knowledge of the continental arc. *American Journal of Science*, 275 (1), Pp. 1-44.
- Means, W.D., 1994. Rotational quantities in homogeneous flow and the development of smallscale structure. *Journal of Structural Geology*, 16, Pp. 437-445.
- Ni, J., Barazangi, M., 1984. Seismotectonics of the Himalayan Collision Zone: Geometry of the underthrusting Indian Plate beneath the Himalaya. *Journal of Geophysical Research: Solid Earth*, 89, Pp. 1147-1163.
- Passchier, C.W., Trouw, R.A., 2005. *Microtectonics*. Berlin: Springer-Verlag.
- Paudyal, K.R., Paudel, L.P., 2013. Geological study and root zone interpretation of the Kahun Klippe, Tanahun, and central Nepal. *Himalayan Geology*, 34 (2), Pp. 93-106.
- Ramsay, J.G., 1967. *Folding and Fracturing of Rocks*. New York: Mc Graw Hill Book Company.
- Ramsay, J.G., Huber, M.I., 1983. *The Techniques of Modern Structural Geology*. London: Academic Press.
- Sakai, H., 1983. Geology of the Tansen Group of the Lesser Himalaya in Nepal. *Memorie of Faculty of science, Kyushu University, Ser.D (Geology)*, 25 (1), Pp. 27-74.
- Sakai, H., 1985. Geology of the Tansen Group of the Lesser Himalaya in Nepal. *Memorie of Faculty of science, Kyushu University, Ser.D (Geology)*, 25 (3), Pp. 337-397.
- Schelling, D., Arita, K., 1991. Thrust tectonics, crustal shortening, and the structure of the far-eastern Nepal Himalaya. *Tectonics*, 10 (5), Pp. 851-862.
- Stöcklin, J., 1980. Geology of Nepal and its regional frame: Thirty-third William Smith Lecture. *Journal of the Geological Society of London*, 137 (1), Pp. 1-34.
- Stöcklin, J., Bhattarai, K., 1977. In *Himalaya Report Geology of Kathmandu Area and Central Mahabharat Range Nepal*. Department of Mines and Geology Kathmandu, Nepal.
- Tikoff, B., Fossen, H., 1995. The Limitations of Three-Dimensional kinematic vorticity analysis. *Journal of Structural Geology*, 12, Pp. 1771-1784.
- Xypolias, P., 2010. Vorticity Analysis in Shear Zones: A Review of Methods and Applications. *Journal of Structural Geology*, 32 (12), Pp. 2072-2092.
- Yin, A., 2006. Cenozoic tectonic evolution of the Himalayan orogen as constrained by along-strike variation of structural geometry, exhumation history, and foreland sedimentation. *Earth Science Review*, 76, Pp. 1-131.

